PTE/105509-4/2022

DOCTORAL SCHOOL OF HEALTH SCIENCES
UNIVERSITY OF PÉCS
FACULTY OF HEALTH SCIENCES

HEAD OF THE DOCTORAL SCHOOL:
PROF DR JÓZSEF BÓDIS MD, PhD, DSc

ANDRÁS GYULA KEDVES

HIGH-DOSE RADIOTHERAPY PROCEDURES REQUIRING PRECISION, MULTIMODAL IMAGING

PHD DISSERTATION

PROGRAMME-6 ONCOLOGY - HEALTH SCIENCES
PROGRAMME LEADER: PROF DR ISTVÁN KISS MD, PhD, DSc
SUB-PROGRAMME-6/2: DIAGNOSTIC MEDICAL IMAGING
SUB-PROGRAMME LEADER: PROF DR PÉTER BOGNER MD, PhD

SUPERVISORS:
DR HABIL ÁRPÁD KOVÁCS MD, PhD
DR HABIL FERENC LAKOSI MD, PhD

PÉCS, 2022

Table of contents

Abbreviations

ADC_{mean}: Average Mean Apparent Diffusion Coefficient

ADC_{min}: Minimum Apparent Diffusion Coefficient

AJCC: American Joint Committee on Cancer.

BT: brachytherapy

CBCT: cone beam computer tomography

CE: contrast enhanced

CCRT: concomitant chemo-radiation

CCS: cancer-specific

CovP: coverage probability

CR: Complete Remission

CRT: Chemoradiotherapy

CT: computed tomography

CTCAE 4.0: Common Terminology Criteria for Adverse Events 4.0.

CTV: clinical target volume

CTV-E: elective target volume

CTV-N_x: clinical target volume particular positive lymph node

DVH: dose-volume histogram

DF: distant failure

DRFS: distant recurrence-free survival

DW(I): Diffusion-weighted (imaging)

EBRT: external beam radiation therapy

EMBRACE: IntErnational magnetic resonance imaging-guided BRAchytherapy in CErvical cancer

EORTC: European Organization for Research and Treatment of Cancer

EP: Echo Planar

EQD2: equivalent dose in 2-Gy fractions

^{18}F-FDG: 2-Deoxy-2-[18F]fluoro-D-glucose

FDG: Fluorodeoxyglucose

FIGO: Fédération Internationale de Gynécologie et d'Obstétrique

FOV: Field of View

FUP: follow up

FS: Fat Suppression

Fx: fractions

gastrointestinal (GI) and

GU: genito-urinary toxicity

GTV: gross tumor volume

GTV-N_x: gross tumor volume particular positive lymph node

Gy: gray

IC/IS HDRBT: intracavital/interstitial high dose rate brachytherapy

IGRT: image-guided radiotherapy

IRB: Local Ethics Committee and the Institutional Review Board

HT: hematological toxicity

HIV: human immunodeficiency virus

H&N: Head and Neck

HNSCC: Head and Neck Squamous Cell Carcinoma

HPV: human papillomavirus

HT: hematological

ICRU: The International Commission on Radiation Units and Measurements

IGABT: image guided adaptive brachytherapy

ITV: internal target volume

ITV45: internal target volume for 45 gray

KSH: Hungarian Central Statistical Office / Központi Statisztikai Hivatal

KWT: Kruskal–Wallis tests

LACC: locally advanced cervical cancer

LF: local failure

LRFS: local failure-free survival

mCR: complete metabolic regression

MRAC: magnetic resonance-based attenuation correction

MRI: magnetic resonance imaging

MTV: Metabolic Tumor Volume

NCR: Non-Complete Remission

N+: nodal metastases

NF: nodal failure

OARs: organs at risk

OS: overall survival

OTT: overall treatment time

PAN: para-aortic lymph nodes

PACS: picture archiving and communication system

PAO: paraaortic

PERCIST: Positron Emission Response Criteria in Solid Tumors

PET/CT: positron emission tomography-computed tomography

PET/MR: Positron Emission Tomography/Magnetic Resonance Imaging

Pts: patients

PTV: planning target volume

PTV45: planning target volume for 45 Gy

PTV-N_x: planning target volume particular positive lymph node

ROI: Region of Interest

RRFS: regional failure-free survival

RT: radiotherapy

SD: standard deviation

SIB-N: simultaneous integrated nodal boost

SUV_{max}: Maximum Standardized Uptake Value

SUL_{peak}: Peak Lean Body Mass Corrected SUV Uptake Value

TE: Time of Echo

TI: Time of Inversion Recovery

TLG: Total Lesion Glycolysis

TNM: Tumor, Node, Metastasis

TR: Time of Repetition

TSE: Turbo Spin Echo

UICC: Union for International Cancer Control

US: Ultrasound

VMAT: volumetric arc therapy

VOI: Volume of Interest

Dissertation outlines

In this dissertation we studied the use of multimodality-based high dose radiotherapy procedures in cervical and head and neck cancer.

Our first aim was to present our experiences with the CovP SIB-N focusing on clinical outcome and nodal volume changes measured on CBCT during treatment. Our results confirm an excellent 2-year clinical efficacy without nodal failures besides and minimal severe morbidity. During the evaluation of 650 CBCTs a volume dependent regression could be observed which might allow for early dose adaptation strategies in the future. - *Retrospective validation of coverage probability based simultaneous integrated nodal boost in locally advanced cervical cancer: a mono-institutional analysis*

Our second aim was to report on the pretreatment PET/MR based PET and MR-Diffusion weighted imaging (DWI) parameters (SUV_{max}, SUL_{peak}, MTV, TLG, ADC_{mean}) role in predicting outcome at HNSCC patients treated with single 18 F-FDG injection dual imaging acquisition PET/MR based chemoradiotherapy. Our finding implies a new perspective of HNSCC treatment planning (with single tracer injection dual imaging protocol) which will be a crutch for the diagnostic physicians to prescribe the best therapy patient tailored. - *Predictive value of diffusion, glucose metabolism parameters of PET/MR in patients with head and neck squamous cell carcinoma treated with chemoradiotherapy.*

Introduction

Cervical cancer

Epidemiology

Cervical cancer is one of the most common cancers in women around the world, accounting for 6% of all cancers in women. With the wide spread of gynecological screening and the treatment of preinvasive disease, cervical cancer shows a decreasing incidence[1]. 10 years ago, cervical cancer ranked as the third most common cancer among women worldwide. However, in 42 low-resource countries, it was the most common cancer in women[2]. Cervical cancer is the fourth most frequently diagnosed cancer and the fourth leading cause of cancer death in women, with an estimated 604,000 new cases and 342,000 deaths worldwide in 2020 (**Figure 1**). According to GLOBOCAN estimates from 2008, there were about 530,000 cervical cancer cases and 275,000 deaths worldwide, with 85 percent of incidences happening in developing countries. The estimated new cases and deaths are decreasing as well in Western Europe and North America (**Figure 2).**

Although mortality from cervical cancer in Hungary decreased by 35 cases per year between 1999 and 2003, according to a comprehensive study published by the National Institute of Oncology in 2005, the incidence of the disease in 2001-2004 with 5051 newly registered patients per year is still on 8. position[3]. According to Nemzeti Rákregiszter, 408 people died of cervical cancer in 2018[4].

The prognosis of the disease at the time of diagnosis has a significant impact on the prognosis. The current fatality rate is significantly higher than it should be because the vast majority (more than 90%) of these cases may and should be recognized early through the use of Pap smear[5].

With 12 oncogenic forms recognized as category 1 carcinogens by the International Agency for Research on Cancer Monographs, human papillomavirus (HPV) is a required but not sufficient cause of cervical cancer. Some sexually transmitted illnesses (HIV and Chlamydia trachomatis), smoking, a higher number of births, and long-term use of oral contraceptives are also essential cofactors[6].

FIGO stages IA, IB, and IIA cervical cancers have traditionally been considered early disease, while FIGO stages IIB, IIIA, IIIB, IVA, and IVB cervical cancers have

traditionally been considered advanced disease. This gave distinct prognostic groups and numbers a simple approach to decide on and implement uniform treatment plans for different stages (**Appendix 1**).

Risk factors

Prostate tumors are classified into three or four groups according to their tendency to recur: low-, medium-, high-, and very high-risk tumors. The classification is based on the following independent prognostic characteristics: pre-treatment prostate-specific antigen value (iPSA), clinical stage and the degree of histological differentiation, i.e. the Gleason score (GS)[7,8] (**Appendix 2**). There is no consensus on the formation of risk groups, different classifications are accepted[9,10]. Multidisciplinary treatment of prostate tumors (surgery, radiation therapy, antihormonal treatment, chemotherapy, biological therapies, active surveillance) is carried out according to risk groups worldwide.

This consideration relates to a minor disadvantage of surgical treatment as the first step in the complex management of cervical cancer, because surgery is still the preferred method of treatment for early-stage cervical cancer, and the complex oncological treatment of advanced disease is based on a combination of external irradiation and brachytherapy with concurrent chemotherapy[11]. Cervical cancers are still of great scientific interest[12].

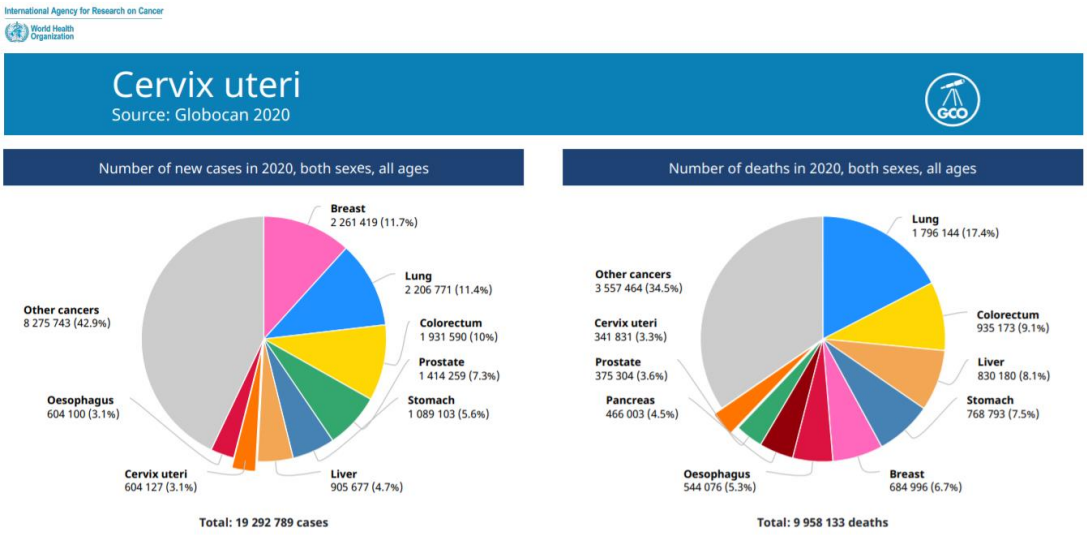

Figure 1. *Number of new cases and number of death of cervix uteri on pie charts. Source: Globoscan 2020. https://gco.iarc.fr*

Head and neck cancer

Epidemiology

Head and neck cancers are a diverse collection of cancers that are physically similar but varied in terms of genesis, histology, diagnostic methods, and therapeutic options. Squamous cell carcinomas account for 91% of all H&N cancers, sarcomas for 2%, and adenocarcinomas, melanomas, and unspecified tumors for the remaining 7%. (European crude and age-adjusted incidence by cancer, years of diagnosis 2000 and 2007 analysis based on 83 population-based cancer registries * 2014). Squamous cell carcinoma of the head and neck (HNSCC) includes cancers of the lip, oral cavity, hypopharynx, oropharynx, nasopharynx, and larynx. Most head and neck cancers are known risk factors for alcohol and tobacco use, and incidence rates have been reported to be greater in areas with high rates of alcohol and cigarette use. (2017, Society for Medical Oncology) [13]

In 2017, the Global Burden of Disease estimated that 890,000 new head and neck cancers (HNCs) were diagnosed in the world, accounting for 5.3 percent of all cancers[14]. According to the most recent epidemiological studies, HNCs are responsible for 507,000 fatalities per year, accounting for 5.3 percent of all cancer deaths[15]. The International Agency for Cancer Research (IARC) claims that, there were a total of 70,454 new cancer cases in Hungary in 2018, with HNC accounting for 6,772 (9.6%) of all new cancer cases[16]. In Hungary, all types of malignancies were the second greatest cause of death behind cardiovascular illnesses, with 33,010 fatalities[17].

The death rate of head and neck malignancies has increased dramatically during the 1970s, according to data from the Hungarian Central Statistical Office (KSH). The number of people diagnosed with these tumors has tripled, and their fatality rate has nearly quadrupled[18].

Risk factors

The two most significant risk factors for cancer are smoking and drinking[19]. Head and neck cancer risk factors include Epstein-Barr virus (EBV) infection and human papillomavirus (HPV) infection (nasopharyngeal cancers in Asia)[20]. Another risk factor for oral cancer is the herpes simplex virus (HSV), albeit this association is weaker than that of EBV or HPV[21]. Head and neck cancer incidence may increase by three times due

to immunodeficiency, which is also a significant risk factor[22]. Along with other, less significant risk factors include occupational exposure to radiation, hereditary factors, chewing betel nuts, poor oral hygiene, and periodontal disease, which has been related to oral cancer, that may contribute to the development of HNC[23,24,25].

Nowadays, there are numerous studies investigating head and neck cancers in our country[26, 27,28,29,30,31].

Cancer incidence and mortality statistics worldwide and by region												
	Incidence						Mortality					
	Both sexes		Males		Females		Both sexes		Males		Females	
	New cases	Cum. risk 0-74 (%)	New cases	Cum. risk 0-74 (%)	New cases	Cum. risk 0-74 (%)	Deaths	Cum. risk 0-74 (%)	Deaths	Cum. risk 0-74 (%)	Deaths	Cum. risk 0-74 (%)
Eastern Africa	54 560	4.46	-	-	54 560	4.46	36 497	3.36	-	-	36 497	3.36
Middle Africa	15 646	3.56	-	-	15 646	3.56	10 572	2.66	-	-	10 572	2.66
Northern Africa	6 971	0.72	-	-	6 971	0.72	4 033	0.46	-	-	4 033	0.46
Southern Africa	12 333	3.70	-	-	12 333	3.70	6 867	2.21	-	-	6 867	2.21
Western Africa	27 806	2.48	-	-	27 806	2.48	18 776	1.88	-	-	18 776	1.88
Caribbean	3 857	1.37	-	-	3 857	1.37	2 495	0.89	-	-	2 495	0.89
Central America	13 848	1.39	-	-	13 848	1.39	6 866	0.74	-	-	6 866	0.74
South America	41 734	1.59	-	-	41 734	1.59	22 221	0.82	-	-	22 221	0.82
Northern America	14 971	0.59	-	-	14 971	0.59	6 343	0.22	-	-	6 343	0.22
Eastern Asia	129 567	1.08	-	-	129 567	1.08	66 436	0.57	-	-	66 436	0.57
South-Eastern Asia	68 623	1.91	-	-	68 623	1.91	38 530	1.16	-	-	38 530	1.16
South-Central Asia	148 128	1.71	-	-	148 128	1.71	91 985	1.10	-	-	91 985	1.10
Western Asia	5 402	0.45	-	-	5 402	0.45	2 951	0.27	-	-	2 951	0.27
Central and Eastern Europe	32 348	1.42	-	-	32 348	1.42	15 854	0.65	-	-	15 854	0.65
Western Europe	10 102	0.67	-	-	10 102	0.67	4 296	0.22	-	-	4 296	0.22
Southern Europe	9 053	0.76	-	-	9 053	0.76	3 705	0.25	-	-	3 705	0.25
Northern Europe	6 666	0.90	-	-	6 666	0.90	2 134	0.22	-	-	2 134	0.22
Australia and New Zealand	1 094	0.52	-	-	1 094	0.52	409	0.16	-	-	409	0.16
Melanesia	1 330	2.64	-	-	1 330	2.64	818	1.84	-	-	818	1.84
Polynesia	35	1.06	-	-	35	1.06	19	0.58	-	-	19	0.58
Micronesia	53	1.97	-	-	53	1.97	24	0.97	-	-	24	0.97
Low HDI	81 922	3.00	-	-	81 922	3.00	56 167	2.31	-	-	56 167	2.31
Medium HDI	182 866	1.83	-	-	182 866	1.83	113 149	1.19	-	-	113 149	1.19
High HDI	240 400	1.30	-	-	240 400	1.30	129 444	0.74	-	-	129 444	0.74
Very high HDI	98 675	0.88	-	-	98 675	0.88	42 920	0.33	-	-	42 920	0.33
World	604 127	1.39	-	-	604 127	1.39	341 831	0.82	-	-	341 831	0.82

Figure 2 *Cervix uteri incidence and mortality statistics worldwide and by region. Source Globoscan 2020. https://gco.iarc.fr*

Study 1

Retrospective validation of coverage probability based simultaneous integrated nodal boost in locally advanced cervical cancer: a mono-institutional analysis

Introduction

Patients with locally advanced cervical cancer (LACC) treated with concomitant chemo-radiation (CCRT) and image-guided adaptive brachytherapy (IGABT) have outstanding results[32,33,34,35,36,37,38,39,40,41]. While local control reaches 86-97% with IGABT, nodal and distant failures (DF) become the dominant causes of treatment failure, leading to poor overall survival (OS), especially for patients with nodal metastases (N+)[34,38,42].

In the EMBRACE study (IntErnational Magnetic resonance imaging-guided BRAchytherapy in CErvical cancer) overall nodal failure (NF) was 11%, including 7% and 16% for N- and N+ patients[43]. Forty percent of NFs were located inside the elective target volume (39% of which in paraaortic node (PAN)) and 35% inside the nodal boost volume. The actuarial 3-and 5-year nodal control rate was 87% (92% (N-) vs. 82% (N+)) and 86%, respectively[43]. The retroEMBRACE study reported a pelvic failure rate of 13% and a pelvic NF rate of 6%[40]. A recent paper showed a 3-year NF rate of 21% with 69% overall survival (OS) with 60 Gy simultaneous integrated nodal boost (SIB-N) without serious morbidity[44].

The EMBRACE II study introduced the Coverage probability (CovP) based simultaneous integrated nodal boost (SIB-N) concept, which allows for a relaxed planning aim at the edge of the nodal planning target volume (PTV-N, 90% of the prescribed dose), with a full dose with hot spots within nodal gross tumor volume (GTV-N) where regression is expected. Controlled underdosage at the edge of the PTV-N and targeted dose escalation at the center are aimed to reduce high dose delivery to adjacent organs at risk (OARs)[45,46,47,48], while maximizing nodal control. However, these dosimetric advantages come with the potential risk of geographic misses, such as internal nodal movement or positioning errors when PAN-RT is given[45]. Ramlov et al. demonstrated that geographic misses have only mild dosimetric impact for pelvic CovP-SIB-N, but few data were presented with PAN SIB-N[45]. Moreover, published results on clinical outcome and nodal volume changes with CovP SIB-N in LACC patients are very limited[46].

These motives led to this retrospective cohort analysis, which aims to present (1) CBCT verification of nodes hit with CovP SIB-N (2) their nodal regression during EBRT and (3) 2-year clinical outcome.

Material and methods

Patients

Between January 2016 and November 2020 sixty-five biopsy-proven LACC patients were treated with definitive RT±CT followed by IGABT, including 33 patients with nodal disease. In the absence of voluminous lymph node(s) and/or very close vicinity of primary or mobile organs (bladder, rectum) CovP-SIB-N was the treatment of choice, which was the case in 29 patients. Three patients showed ulta-early (<6 weeks) unusual distant progression (subcutaneous, peritoneal, hepatic) and were excluded from this study. Analysis was performed using data from 26 LACC patients treated with CovP-SIB-N technique with weekly cisplatin (40 mg/m²), followed by IGABT.

Staging consisted of gynecological examination according to Fédération Internationale de Gynécologie et d'Obstétrique (FIGO), a thoraco-abdominal scan and 3T abdominal-pelvic magnetic resonance imaging (MRI) (Biograph mMR, Siemens Healthcare GmbH., Erlangen, Germany) for all patients completed by a whole-body 18F-fluorodeoxyglucose positron-emission tomography-computed tomography (18FDG PET-CT, Biograph 64, Siemens Healthcare GmbH., Erlangen, Germany). Cystoscopy or rectoscopy was added if organ infiltration was suspected.

Nodes were considered pathological according to EMBRACE II criteria: FDG-PET positive or short axis >1cm on CT or MRI and/or short axis between 0.5 and 1.0 cm on MRI with pathological morphology (irregular border, high signal intensity and/or round shape).

Contouring and planning followed the EMBRACE II protocol[47] for regional irradiation. In summary, CT and MRI scans were obtained with full and empty bladder conditions to assess movement patterns and to create internal target volume (ITV). All scans were co-registered in the Eclipse Treatment Planning System (Eclipse v13, Varian, Palo Alto, CA, USA). Pathological nodes were contoured (GTV-N) on MRI and CTs, then merged to form CTV-N (clinical target volume). The elective target volume (CTV-E) included pelvic lymph-nodes up to the aortic bifurcation. If >2 pathological nodes were identified, or if node(s) were located at the typical iliac vessels or higher, PAN to the level

of the renal vessels was systematically included. An ITV for 45 Gy (ITV45) including CTV-E and CTV-N was created using information from co-registered images. PTV45 (PTV for 45 Gy) and PTV-N_x were created using a 5-mm isotropic margin around ITV45 and CTV-N[16].

Treatment planning consisted of two 6MV volumetric arc therapy beams (TrueBeam 2.5, Palo Alto, CA, USA). Planning aims for elective and SIB-N volumes were the following: PTV45: V42.75 Gy >98%, CTV-N and PTV-N: D98≥90%, CTV-N D98≥100% and CTV-N D50≥102% of the prescribed dose, which was 55 Gy/25 fx to nodes in the small pelvis and 57.5 Gy/25 fx to nodes further away. Treatment verification consisted of daily CBCT with bony anatomy match including extended CBCT for PAN SIB-N.

Boosted nodes were contoured on each CBCT (GTV-N_{CBCT}) and were assessed for coverage by PTV-N. Target coverage was evaluated by comparing individual nodal delineations with the relevant PTV-N. In patients with insufficient coverage the dose to 98% (D98%), 50% (D50%) of each GTV-N_{CBCT} was assessed according to the planning CT dose distribution by propagating the individual GTV-N_{CBCT} via rigid bony registration to the planning CT. The accumulated D98%, D50% were calculated as the mean of each DVH parameter across all CBCT contours in a given patient.

The high-dose-rate (HDR) BT schedule included 2 to 4 fractions in one or two applications. Before the introduction of the interstitial needles and in cases with distant parametrial spread where target coverage would have been compromised even with parallel needles, external beam sequential boost was given to the primary tumor up to 60 Gy. These patients were re-planned with empty and full bladder conditions and the target volume was the adapted high-risk CTV. Thus two fractionation schedules were used for the primary tumor: 60 Gy+2x7 Gy HDRBT (n=5) or 45 Gy+4x7 Gy (n=21). Target and OAR delineation and dose reporting for IGABT were based on the International Commission on Radiation Units and Measurements (ICRU) Report 89[49].

Patients were followed with gynecological examination every three months in the 1st year, twice a year in the second and third year, and once a year afterward. Patients also had an MRI at three months and PET-CT where it was possible, repeated when relapse was suspected. Both acute hematological (HT)/renal toxicity and late gastrointestinal (GI) and genito-urinary (GU) toxicity were scored using the Common Terminology Criteria

for Adverse Events (CTCAE 4.0) and documented in case of ≥Grade (Gr.) 3 due to the retrospective nature of the study.

Complete clinical remission was defined as no evidence of disease 3 months after completion of treatment. Crude and 2-year actuarial rates of local failure-free (LRFS), distant metastasis-free (DMFS), regional failure-free (RRFS), cancer-specific (CCS), and OS were calculated and described by the Aalen-Johansen competing risk assessment[50]. All follow-up (FUP) were calculated from the end of treatment.

Descriptive statistics were given for clinical variables and dose-volume parameters. Statistical evaluation was performed using scipy (1.6.3) and lifelines (0.26.0) python (3.7) packages (Python Software Foundation, Beaverton OR, USA).

Results

Patient-, tumor- and treatment characteristics

Patient cohort characteristics are presented in **Table 1**. The dominant FIGO stage was IIB (54%), with >50% cases with initial tumor size ≥ 5 cm. Most patients (96%) had squamous cell cancer. The median overall treatment time (OTT) was 49.5 (range: 31-70) days. Eighty-nine percent of patients received ≥ 4 cycles of cisplatin. Eleven pts received PAN irradiation including two cases with elective intention.

Dose constraints for EBRT CTV-N D98 and PTV-N D98 were achieved in 91% and 83% of the nodes, while for OARs they were fulfilled in ≥ 96% of the cases (**Table 2-3**). Dose-volume parameters for IGABT are presented in (**Table 4**).

In total, 76 nodes (range:1-6/pts, average volume: 3.20 cm^3, r:0.8-25.3) were boosted, 20% at the PAN region (**Table 1**).

All lymph nodes showed regression (**Figure 3**) including 71% with complete or remarkable partial remission during EBRT. There was a trend that smaller lymph nodes achieved diminished volume earlier, than the larger ones (>10 cm^3).

61/76 nodes were unambiguously detectable on CBCT, the remaining ones were outside the CBCT field of view (n=9) or not clearly identifiable (n=6) (i.e. adjacent nodes, bowel air artefacts). The mean GTV_{CBCT} of PAN and pelvic lymph nodes were not significantly different: 5.4 (SD:6.8) cm^3 vs. 4.0 (SD:5.1) cm^3 (p=0.427). In patients with PAN- and pelvic SIB-N the mean reduction in PAN and pelvic nodal size during EBRT was 70% and 75%. During the evaluation of 650 CBCTs, only 3/61 nodes in 5 fractions were not completely covered by the corresponding PTV-N in one patient. All were pelvic nodes. One node had a D98% of 94%, with a D50% of 100%. The volume of this node was 0.8 cm^3 and the node was located close to the round ligament, which with varying uterus position was displaced for 5 fractions. The remaining 2 nodes had D98% >95% with maintained D50%. After a median FUP of 25 months (3-52), there was no NF. There were 4 recurrences/progressions consisting of 2 local failures (LF) and 2 DFs. The 2-years actuarial/crude rates of OS/CSS/DMFS/LFFS were 90/80, 95/88, 100/92, 90/92% respectively, in alignment with the slightly worse competing risk incidence (**Figure 4**).

Each failed patient had PAN disease at diagnosis. Twenty-one patients were alive at the last FUP (80.7%), 3 deaths were cancer-related.

Eleven ≥Gr.3 hematologic side effects (42%) occurred (4 neutropenia, 2 thrombocytopenia 5 anemia) in 9 patients from which 7 received PAN irradiation. One patient developed Gr.2 duodenal ulcers after PAN-RT which fully recovered after conservative treatment. One patient had Gr.3 colitis with accompanying stenosis of the sigmoid colon requiring elective surgical removal at 1-year FUP. MRI suggested a relationship with three SIB-N targets. The patient did not receive external beam boost. Full plan revision (including delineation of sigmoid on each CBCT [**Appendix 3**]) confirmed that dose-limits would have been respected even if the sigmoid colon was in the closest location to SIB-N through 25 fractions (EBRT+HDR-BT, EQD2: D_{2cm3}: 63.8 Gy (ideal:1.8 Gy/fx) vs. 67 Gy (median dose based on individual CBCTs: 1.9 Gy/fx) vs. 74 Gy("worst-case scenario": 2.1 Gy/fx).

Discussion

This study aimed to present our experiences with CovP SIB-N in LACC patients referred for CCRT. After a 2-year median FUP there was no NF either in the boosted or in the elective RT regions. The majority of the nodes were visible on CBCT and 71% of the nodes achieved a diminished volume already during EBRT. Additionally, only one Gr.3 GI event occurred. It should be mentioned that by taking the EMBRACE II guideline into consideration we have given 10% more elective PAN RT than previously, and the average size of boosted nodes was small (3 cm^3).

A positive lymph node both at diagnosis[38,42,43] and as failure is a poor prognostic factor, confirmed by the EMBRACE I study cohort with actuarial 3-year NF of 8% and 18% in the N- and N+ group with >70 % mortality rate in patients with NF. Even though N+ received a median dose of 59 Gy, 12% developed NF within PTV-N. Moreover, 41% were located outside the elective target, including 39% in the PAO region[34]. EMBRACE II addressed these possible limitations for EBRT[41], including two major improvements for nodal irradiation: expansion of CTV-E to the PAN region and the CoV-SIB-N concept. Published literature with CoV-SIB-N is still limited. Lindegaard et al.[33] were the first to demonstrate a pelvic control of 91%, including only one NF within a boosted 1.1 cm^3 node in the small pelvis boosted with 55 Gy/25 fx and two other NFs in the un-irradiated PAN at 9 months median FUP.

RetroEMBRACE[40] data revealed significant correlation between local control and dosage, volume, and OTT for all primary target volumes. It remains unknown whether involved nodes require much higher doses. Ramlov et al.[51] investigated the pattern of nodal failure for N+ patients in function of the individual nodal dose (75 pts, 209 nodal boosts, median dose 62 Gy (EQD2)). Six patients relapsed in boosted area. They did not find correlation between nodal dose and volume[45]. In contrast Bacorro et al.[52] found a nodal dose-volume effect on nodal control probability with increasing benefit of additional doses to higher-volume nodes. These contradictory data should be resolved by a large prospective study.

Investigating lymph node response during treatment on daily CBCTs revealed some additional aspects. First, the image quality of extended CBCT was sufficient to define 80% of SIB-Ns which is in line with the results of Ramlov et al.[45]. Similarly to

Ramlov[45] and Bacorro et al.[52] we observed a remarkable response of boosted nodes during EBRT which was achieved sooner for the smaller ones (<3 cm^3).

The retrospective nature, small sample size, heterogenous treatment and follow-up are the main limitations of our study.

Conclusion

Still, CovP-SIB-N with daily image guidance resulted in excellent 2-year nodal control and a low rate of late toxicity, with remarkable nodal response during EBRT. Longer follow-up and larger prospective studies such as EMBRACE II are required to confirm this observation. Our experiences encourage the clinical use of CovP-SIB-N in LACC patients.

Figures

Figure 3

Boxplot representation of initial (planning) volume of all (ALL), CBCT-detected (*) para-aortic (PAN) and pelvic (PEL) positive lymph nodes (left), relative volume changes (regression) in function of the fractions for the Q3 (75%), Median (50%) and Q1 (25%) of the cohort.

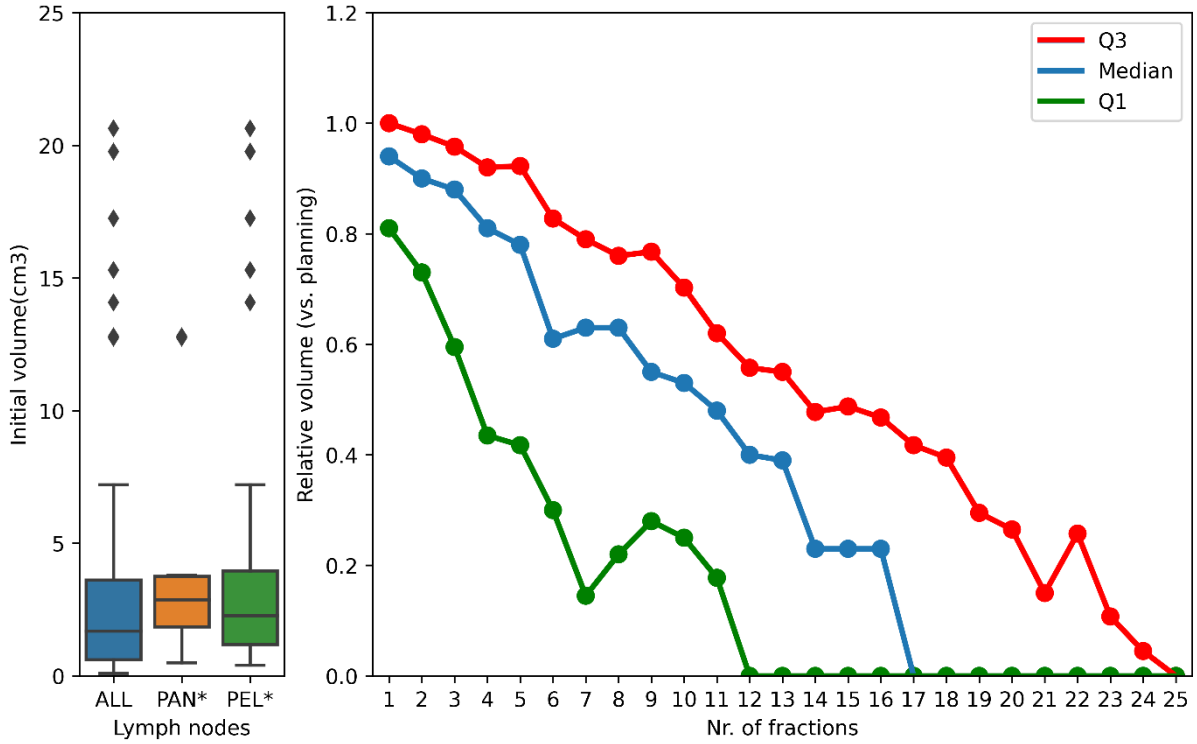

Figure 4

Competing risk analysis for the clinical outcome (OS: overall survival; CSS: cancer-specific survival; LFFS: local failure-free survival; DMFS: distant metastasis-free survival).

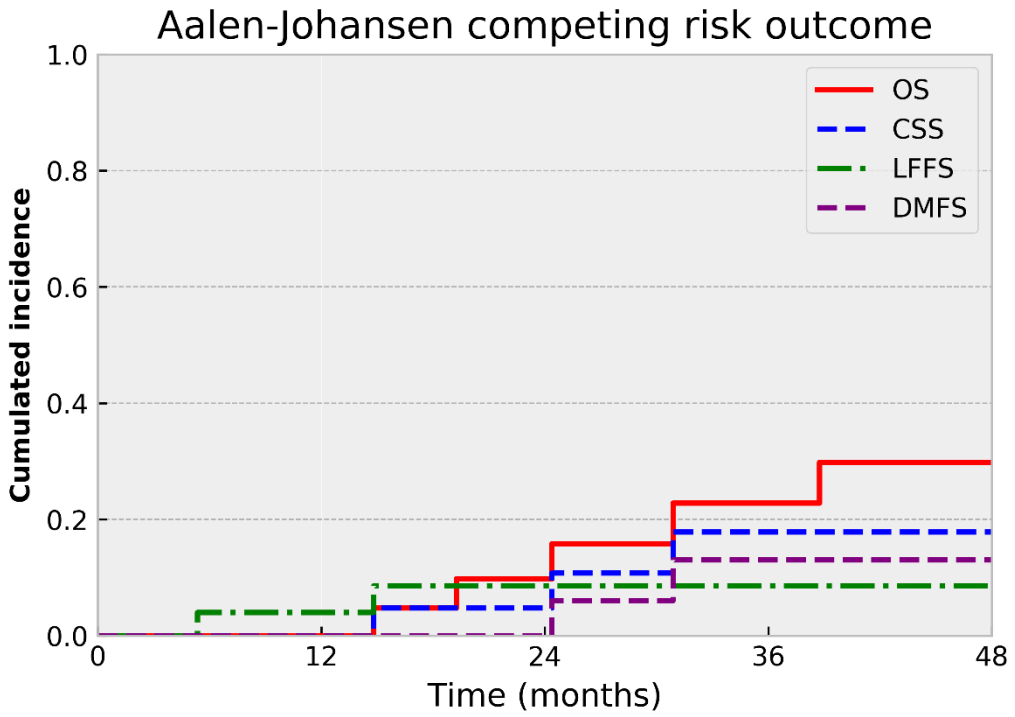

Tables

Table 1

Patient, tumor, and treatment characteristics. Abbreviations: FIGO: Fédération Internationale de Gynécologie et d'Obstétrique; EBRT: external beam radiation therapy.

Characteristics	**Value (%)**
Number of patients	26 (100)
Median age (year)	61±12 (40-76)
FIGO stage IIA/IIB/IIIA/IIIB/IVA	4/17/1/3/1 (15/65/4/12/4)
No. of nodes per patient 1/2/3/>3	5/4/9/8
No. of nodes per localization total	76 (100)
Para-aortic	15 (20)
Common iliac	7 (9)
Parametrial, mesorectal, presacral	3 (4)
Internal iliac	18 (24)
External iliac and obturator	33 (43)
EBRT target	
Pelvis	14 (54)
Pelvis and para-aortic region	11 (42)

Table 2

Dose-volume parameters for coverage probability (CovP) simultaneous integrated nodal boost (SIB-N) for 76 individual nodes. Abbreviations: D50 CTV-N: minimum dose to 50% of the CTV-N volume; D98 CTV-N: minimum dose to 98% of the CTV-N volume; D98 PTV-N: minimum dose to 98% of the PTV-N volume, *in 3 nodes dose was descalated to 55 Gy due to the direct contact with the duodenal loop.

Dose level	**Aim (Gy)**	**55Gy/25fx Prescribed dose (Gy)**		**Aim (Gy)**	**57.5Gy/25fx Prescribed dose (Gy)**	
No.of nodes		64			12*	
		Mean	Range		Mean	Range
D50 CTV-N, Gy	≥ 56.1	56.83	(53.86-59.65)	≥ 58.7	60.030	(59.65-60.78)
D98 CTV-N, Gy	≥ 55	55.42	(52.42-58.27)	≥ 57.5	58.852	(58.0-60.30)
D98 PTV-N, Gy	≥ 49.5	50.34	(42.51-54.17)	≥ 51.8	53.169	(51.82-55.35)

Table 3

Dose-volume parameters for CovP-SIB-N for OARs.

OARs	Aim		Prescribed dose (Gy)			
			Mean	Median	Min	Max
Bowel	Dmax (Gy)	<57.5	52	53	47	61
Rectum	Dmax (Gy)	<57.5	48	47	46	52
Sigmoid	Dmax (Gy)	<57.5	51	50	47	57
Bladder	Dmax (Gy)	<57.5	49	49	47	58
Bowel	V40Gy [cm³]	<250	191	155	45	699
Bowel	V30Gy [cm³]	<500	410	359	144	1072
Rectum	V30Gy [% of volume]	<95	85	90	60	100
Rectum	V40Gy [% of volume]	<85	67	70	37	100
Bladder	V30Gy [% of volume]	<85	81	82	38	98
Bladder	V40Gy [% of volume]	<75	62	64	23	86
Left Kidney	Mean dose (Gy)	<10	6	7	0	14
Right Kidney	Mean dose (Gy)	<10	6	7	1	12
SpinalCord	Dmax (Gy)	<48	22	31	1	39
Right Femur	Dmax (Gy)	<50	40	41	33	46
Left Femur	Dmax (Gy)	<50	40	40	33	46

Table 4

Dose-volume parameters for image guided adaptive brachytherapy (IGABT) in Doses are calculated as equivalent dose in 2 Gy fractions (EQD2) of external beam radiation therapy (EBRT) and BT combined using the linear quadric model with α/β=10 for tumor and α/β=3 for organs at risk. Abbreviations: D98 CTV_{IR}: the dose to 98% of the intermediate-risk clinical target volume; D98 CTV_{HR}: the dose to 98% of the high-risk clinical target volume; D90 CTV_{HR}: the dose to 90% of the high-risk clinical target volume; D_{2cm^3}: the lowest dose evaluated in the maximally exposed $2cm^3$ of the organ; SD: standard deviation.

	Prescribed total dose (EQD2 Gy)	
	Mean	**SD**
D98 CTV_{IR}	58.9	8.8
D98 CTV_{HR}	79.5	5.8
D90 CTV_{HR}	85.6	6.4
Bladder D_{2cm^3}	79.9	6.5
Rectum D_{2cm^3}	59.1	6.9
Sigmoid D_{2cm^3}	63.0	4.8

Study 2

Predictive value of diffusion, glucose metabolism parameters of PET/MR in patients with head and neck squamous cell carcinoma treated with chemoradiotherapy

Introduction

Head and neck carcinomas are the sixth most common cancers, nowadays. These carcinomas make up 6% of all new cancer cases recorded yearly[53,54]. The majority of head and neck carcinomas belong to the histopathological group of squamous cell carcinoma of the head and neck (HNSCC)[55].

The main clinical staging components for diagnosing HNSCC is the endoscopy, but conventional radiological staging methods, such as Computed Tomography (CT) and Magnetic Resonance Imaging (MRI) have proven more accurate and informative in setting up a diagnosis[56].

Beyond these conventional imaging methods, hybrid imaging has also shown an outstanding staging ability, particularly in detecting or characterizing head and neck cancers[57]. Hybrid imaging, such as Positron Emission Tomography/Computed Tomography (PET/CT) or PET/MR, is an imaging solution that could be used simultaneously with anatomical information to provide metabolic data (with a ^{18}F-FDG: 2-Deoxy-2-[18F]fluoro-D-glucose [^{18}F-FDG] tracer). With the information obtained using hybrid imaging, oncological practice could conduct many diagnostic or therapeutic procedures, for example, whole-body staging/restaging, irradiation planning or even the evaluation of the disease prognosis[58,59].

To characterize HNSCC, it is essential to use PET imaging with an ^{18}F-FDG tracer. Multiparametric data obtained from the ^{18}F-FDG PET evaluation was not only linked with histopathologically-confirmed tumor properties, but also connected with PET/MR parameters (such as the apparent diffusion coefficient, ADC, derived from diffusion-weighted imaging [DWI] examinations, the maximum standardized uptake value [SUV_{max}], and the peak lean body mass corrected, SUV_{max} [SUL_{peak}]), and treatment-associated failure, locoregional recurrence, and death[60]. In many malignancies, ^{18}F-FDG accumulation (in the most common form, known as SUV) appears to be a good indicator of disease aggressiveness[61]. There are numerous studies aimed at the utility of FDG PET parameters in predicting response to CRT in head and neck cancer specifically[62,63].

The PET/MR method combined with conventional contrast-enhanced (CE) MR sequences is excellent for getting data on anatomical and metabolic conditions, although data on the cellular diffusion of the scanned area could also be derived via DWI methods during the MR acquisition[64]. Besides the clinical and histopathological factors, imaging parameters may provide important prognostic biomarkers in different malignancies[60]. DWI can measure water molecules' movement and the tumor cell density in tissue in vivo[65]. DWI methods could be used for staging HNSCC. In some cases, DWI allows for a more accurate staging method than PET/CT (e.g. evaluating cN0) [66]. DWI-derived variables, such as ADC, may have a prognostic and predictive value that related to the post-therapeutic status of the disease and the outcome of chemoradiotherapy[67]. To investigate the predictive value of ADC, scans must be performed before and after treatment. According to the results using this method, ADC could be an indicator of locoregional failure, which is a component of the treatment response. The ADC mean values (ADC_{mean}) are therefore possible parameters for prediction, per the suggestion of Martens et al.[68]. Leifels et al. found that tumor metabolism, cellularity, and perfusion show complex relationships in HNSCC. Furthermore, these associations depend on tumor grading[69].

Moreover, Metabolic Tumor Volume (MTV), and Total Lesion Glycolysis (TLG) seem to be predictors of the postoperative survival of patients that have been diagnosed via PET/CT, with MTV seeming to be a better predictor than TLG[70]. Overall, there are numerous studies aimed at the utility of FDG PET parameters in predicting response to CRT in head and neck cancer specifically[62,63].

This study aimed to determine the best predictors for the treatment outcome of patients diagnosed using a single tracer injection dual imaging acquisition protocol in PET/MR from a set of previously described parameters (SUV_{max}, SUL_{peak}, ADC_{mean}, MTV, TLG). This study also aimed to evaluate the connection between the possible above parameters that prove to be the most predictive of the HNSCC outcome.

Materials and methods

Patients and treatment

Informed consent was waived by the Local Ethics Committee and the Institutional Review Board (IRB). Between October 2015 and May 2019, 68 pathologically confirmed, HNSCC patients (male: female ratio of 3:1) with a median age of 61 ± 8 years (range, 46–87) were enrolled in the current retrospective study. All patients underwent 3D-fused ^{18}F-FDG PET/CT Volumetric Modulated Arc Therapy (VMAT)-based, definitive image-guided irradiation (IGRT, with a daily cone-beam CT) and concomitant chemotherapy (with 40 mg/ml cisplatin protocol weekly) up to 70 Gy in Dr. József Baka Diagnostic, Radiation Oncology, Research, and Teaching Center, "Moritz Kaposi" Teaching Hospital, Kaposvár, Hungary. Exclusion criteria were: (1) Patients with second primary malignancy; (2) Patients with previous history of surgery; and (3) Patients with recurrent primary tumors (**Figure 5**).

All patients underwent pretreatment staging (during the planning process 4 weeks before treatment) and post-treatment (12 weeks after treatment) PET/CT and PET/MR for a short-term follow up. Per the 8th edition of the Union for International Cancer Control (UICC) TNM Project 8th TNM staging system, 5/68 (8%) patients had T1 disease, 21 (31%) patients had T2 disease, 23 (33%) patients had T3 disease, and 19 (28%) patients had T4 disease. Meanwhile, 33 of the patients had a histopathologically-confirmed (supported by ultrasound [US] guided biopsy) locoregional lymph node, while 35 showed an absence of metastatic lymphoid glands. Grades distribution were as follow: G1 (n = 15); G2 (n = 35); and G3 (n = 18). N category was as follow: N0 (n =35); N1 (n = 19); N2 (n = 9); and N 3 (n = 5).

Primary tumor localizations were: pharyngeal (n = 32), sub-localized into 7 patients nasopharyngeal, 13 patients oropharyngeal and 12 patients with hypopharyngeal. Laryngeal (n = 36), sub-localized into 26 with supraglottic, 4 glottic and 6 subglottic. The epidemiology data specific to the tumor and lymph node and the response to therapy are summarized in **Table 5.**

PET/MR acquisition

Examinations were performed using a hybrid PET/MR scanner (Biograph mMR, Siemens Healthcare GmbH., Erlangen, Germany). Blood glucose level was checked before tracer injection to ensure the patients were euglycemic. The patients received

intravenous administration of 4 MBq/kg activity of ^{18}F-FDG. Then, PET/CT (Truepoint 64, Siemens Healthcare GmbH., Erlangen, Germany) was performed, using FDG initially injected for PET/CT (60 ± 10 minutes of the uptake period) before PET/MR (15 ± 5 minutes after PET/CT). Further tracer injection was not applied for PET/MR (single tracer injection dual imaging acquisition protocol). After proper patient preparation (removal of metal implants, hearing aids, metal objects in the region), images were obtained of the head and neck position using dedicated coils. Thus, only PET/MR parameters were included in the research.

Native MRI sequences were T2-weighted TSE turbo inversion recovery magnitude (TIRM) (TR/TE/TI 3300/37/220 ms, FOV: 240 mm, slice thickness: 3 mm, 224 × 320) coronal, and T1-weighted turbo spin-echo (TSE) (TR/TE 800/12 ms, FOV: 200 mm, slice thickness: 4 mm, 224 × 320), and T1-weighted TSE Dixon fat suppression (FS) (TR/TE 6500/85 ms, FOV: 200 mm, slice thickness: 4 mm, 256 x 320) transversal and acquired without an intravenous contrast agent.

Diffusion-weighted (DW) measurement was done as part of a routine examination. In this case, a 2D spin-echo DWI echo-planar (EP) sequence (FOV: 315 mm, TR: 9900 ms, TE minimum: 70 ms, TI 200 ms, slice thickness: 5mm) was used. An ADC map was automatically generated from the DWI pictures via the implemented software. The restricted diffusion rate was quantified by calculating the apparent diffusion coefficient. To reduce the perfusion effect (on the ADC calculation, a 50 s/mm^2 "b" value was used as the first measurement (the other b values were 800 s/mm^2 and 1000 s/mm^2). Furthermore, an axial Dixon FS T1-weighted TSE sequence and a coronal TSE Dixon FS sequence were conducted after 0.1 mmol per kg of bodyweight contrast material (Gadovist© Bayer Healthcare, Leverkusen, Germany) was injected into the patient (**Figure 6)** The imaging was repeated after the completion of the CRT for therapeutic response assessment.

For PET data collection, a magnetic resonance-based attenuation correction ([MRAC], using a CAIPIRINHA-accelerated T1-weighted Dixon 3D-VIBE sequence) was used for PET attenuation correction, and the wide range bed position PET Emission scan was acquired for 900 seconds with a fixed FOV range (20 cm) and a (172 × 172) matrix without bed movement. An iterative ordered subset expectation maximization (3D OP-OSEM) PET image reconstruction algorithm was used with 3 iterations and 8 subsets,

as well as 4-mm Gaussian filtering settings. PET data was corrected for scatter, random coincidences, and attenuation using the MR data.

Image analysis

Metabolic parameters were calculated using a dedicated Syngo.via (Siemens Medical Solutions, VB20, Siemens Healthcare GmbH., Erlangen, Germany) multimodality image evaluation and post-processing application based on fusioned PET/MR imaging. The SUV_{max}, SUL_{peak}, MTV, and TLG data of the primary head and neck cancers were collected using the volume of interest (VOI) technique. This study was built only on one observer assessment. VOIs were assessed by a nuclear medicine physician, with 15 years of experience. The SUV_{max} represents single voxel activity concentration in a particular lesion with the highest uptake. The SUL_{peak} is defined as a lean body mass normalized-average SUV value measured in a 1 cm^3 volume spheric region of interest (ROI) centered around the hottest point in the tumor foci. For the MTV and TLG definition, the relative threshold at 50% of tumor SUV_{max} was used, as proposed by Deron et al.[71], where MTV represents the volume of the above given VOI while TLG is the product of the VOI average SUL (SUL_{mean}) multiplied by the corresponding MTV.

The localization of lesions was assessed on the ADC map using eRAD PACS Desktop Viewer 8.0 software. This study applied the single slice measurement method, we have chosen the largest and the most homogeneous part of the tumor as a standard for all objects[72]. ROI was placed manually on the most solid part of the tumor, which shows the highest signal intensity on DWI images (hyperintense) and hypointense on ADC map [42,43]. ROIs were measured by a radiologist with 10 years of experience in DWI measurement. Thus, during the ADC measurement, the researchers took precautions, such as excluding areas of gross necrosis from the sample (ROI), while plotting an elliptic ROI[73]. In all lesions, ADC_{mean} was used as a standard measurement unit to minimize the effect of tumor heterogeneity, it also was the standard unit to be used as a reliable parameter, because it reflects the heterogeneity of the tumor in the specified slice and to enable the researcher to distinguish the different entities in the same image[57,58,74] (**Figure 6**).

Clinical evaluation

To evaluate the therapeutic tumor responses based on pre-and post-treatment PET/MR and PET/CT information, the European Organization for Research and

Treatment of Cancer (EORTC)[75] system was used. Two patient groups were established according to the results of the PET/MR therapeutic response evaluation and the clinical follow-up. Furthermore, patient subgroups were also set up, namely, a Complete Remission (CR) group defined as patients with an absence of a viable primary tumor tissue, and a non-Complete Remission (NCR) group defined as patients with any pernicious proliferations including partial response, stable disease, and progressive disease groups [76,77].

Statistical analysis

For all the statistical analyses conducted, R-scripts developed in-house based on the R-software environment for statistical computing (version 3.3.1; R Foundation for Statistical Computing, Vienna, Austria[78]) were used together with ggpubr[79] and summarytools[80] software packages.

The Shapiro-Wilks test [50] was used to check the normality of the measured SUV_{max}, SUL_{peak}, TLG, MTV, and ADC_{mean} data. Since these tests showed non-normality distributions of the SUV_{max} ($p < 0.0001$), SUL_{peak} ($p = 0.0001$), TLG ($p < 0.0001$), and MTV ($p < 0.0001$) in the population, Spearman's correlation coefficient was used to describe the strength of the correlation between the data pairs, and Wilcoxon's rank-sum test was used for group comparison. The estimated parameters were correlated in different tumor subgroups (grade 1-2 and 3) per suggestion of Leifels et al.[69].

Results

A total of 68 patients were enrolled in this study. The patients' characteristics are summarized in **Table 5**. Well-visualized primary lesions were defined in all patients with the initial ^{18}F-FDG PET/MR.

The mean SUV_{max}, SUL_{peak}, TLG and MTV, ADC_{mean} (+ SD) values measured from the patients' primary tumors were 9.05 ± 6.55 (range, 3.43–41.22), 6.95 ± 5.50 (range, 2.91–32.34), 121.48 ± 163.09 (range, 4.72–570.60), 25.88 ± 21.49 cm^3 (range, 1.38–110.52), and 933.34 ± 136.15 10^{-6} mm^2/s (range, 610.29–1337.85), respectively (**Table 6**).

Correlation analysis

Based on the restaging, the PET/MR scans for CR (**Figure 7**) were achieved for 36/68 (53%) patients, while viable tumor was observed in 32/68 (47%) patients.

The results of the correlation analysis are summarized in **Figure 8** No significant correlation between SUV_{max}, SUL_{peak}, TLG, and MTV and the ADC_{mean} for the patients diagnosed using the single tracer injection dual imaging acquisition protocol was noted.

On the next step, in two separated tumor subgroups, the estimated parameters were correlated. In G1/2 tumors, all PET parameters correlated well. (**Table 7**). In G3 tumors, PET parameters also have shown significant correlations. (**Table 8**). Finally, PET imaging based parameters values did not correlate with ADC_{mean} in both groups.

Measured parameters and response

According to Wilcoxon's rank-sum test, no statistically significant difference was found for the ADC_{mean} ($p = 0.88$) of patients that achieved a complete response and subjects with a viable tumor tissue after CRT. Nevertheless, SUV_{max}, SUL_{peak}, TLG, MTV ($p = 0.032$, $p = 0,01$, $p < 0.0001$, $p = 0.0004$) proved to be significantly different between the two different outcome groups (**Figure 9**).

Discussion

The radiotherapy of HNSCC patients based on modern complex oncological treatment is usually combined with chemotherapy and/or surgical resection[81]. HNCs still have a bad overlook in the overall prognosis of the combined treatment modalities. An overall loco-regional recurrence may occur in up to 40% of locally advanced head and neck patients after the first 2 years[82]. Due to the anatomical features of the head and neck region, organ preservation is important to maintain functions and to minimize aesthetic changes[83]. Hoffman et al. raised some attention regarding neoadjuvant treatment strategies for tumor reduction before surgery. They also pointed out the efficacy of CRT and neoadjuvant chemotherapy followed with definitive radiotherapy for advanced HNSCC patients[84].

The study also highlighted the need to accurately predict the outcome of possible treatment options in daily clinical practice. The high mortality rate of advanced HNSCC patients and the precise cancer staging of radical resections are, therefore, essential, as both allow clinicians to select the relevant treatment strategies that could predict the prognosis of the patients[85]. Hence, it is essential to identify the potential predictive indicators for these treatments.

Pretreatment ^{18}F-FDG-PET/MR were evaluated for their predictive value for clinical outcomes. It is crucial to prognosticate the disease response of treatments in the pretreatment period to establish a more aggressive treatment for selected HNSCC patients[59,86].

Overall, in this research we focused on the combined role of DWI and PET imaging parameters for predicting tumor response to therapy in the head and neck region.

In this examination, SUV_{max}, SUL_{peak} MTV, TLG values of HNSCC patients were the predictive factors for determining response to therapy. After CRT, the risk of NCR was significantly higher in patients with high SUV_{max}, SUL_{peak}, MTV, and TLG values than in patients with low SUV_{max}, SUL_{peak}, MTV, and TLG values. Thus, the current results confirm that both TLG and MTV can add valuable information for prediction, further supporting Pak et al.'s finding, which argued that patients who have a higher risk of death and adverse events have high MTV or TLG [87]. Additionally, in the current study, patients diagnosed using a single tracer injection double imaging acquisition protocol in PET/MR, and the non-complex (SUV_{max}, SUL_{peak}) parameters supported this finding as well.

The present study investigated numerous patients treated with CRT and diagnosed with histopathologically-proven HNSCC. Furthermore, the study also investigated the correlations between PET and MRI-DWI parameters that were acquired simultaneously.

Via this approach, these parameters could be used to select a treatment strategy to address the higher SUV_{max}, SUL_{peak}, TLG, and MTV values that indicate a poorer treatment outcome. Therefore, it is worth taking the parameters suggested above into daily routine, especially the ones that significantly predict the patient outcome in daily routines to achieve more patient-tailored therapy.

Several studies found negative associations between SUV_{max} and ADC values[88,89]. However, in our study, no significant linear correlations were found between the investigated parameters. Our results are similar to the results found by Rasmussen et al. Furthermore, when we classified the patients into two different groups based on the primary tumor degree of differentiation, no significant correlations were found. Since we only measured ADC_{mean}.

Contrary to a study by Wong et al., who reported that the ADC was a predictive factor to assess response to chemo-radiotherapy, we couldn't find a significant difference in the post-treatment ADC_{mean} between the two groups, there was no noticeable difference in the ADC values[90].

The simultaneous imaging in PET/MR provides the same bed positions and acquisition at the same time, which leads to more accurate results compared to studies that have examined them separately on individual modalities. Compared to previous studies, this study found that both the parameters (SUV_{max}, SUL_{peak}, MTV, TLG) had predictive values while using the single tracer injection double imaging acquisition protocol. In this research, the SUV_{max}, SUL_{peak}, MTV, TLG values were measured; thus, their predictive value was discovered very first in homogeneously treated head and neck cancer patients.

In contrast, a few limitations must be acknowledged. The first weak point of this study was the retrospective analysis and the single-institute implementation. Moreover, a long term follow-up might be more accurate to determine the therapeutic response. A multi-center and prospective study with more patients could be more representative of the population.

Surov et al. found that combined DWI and PET imaging parameters were useful to predict several histopathological features, which might be more accurate to understand how tumors interact with these imaging modalities, however, our study was included only the conventional parameters, which might be one of the limitations of this research[91]. Despite these limitations, this report provides important contributions to the field because it is the first study to show the predictive value of SUV_{max}, SUL_{peak} MTV, and TLG, in patients with diagnostically-confirmed HNSCC that were diagnosed with single tracer injection dual imaging acquisition. The usefulness of the ^{18}F-FDG PET/MR is important, nevertheless, it has questionable added value, because ADC_{mean} has not shown significant differences between 2 patient groups (CR: n=36 and non-CR: n=32), probably due to the small number of patients (n=68). Besides, this study also reported no correlations between PET and MRI-DWI based parameters. The findings suggest a need for further studies that involve more patients and more PET parameters, as well as wider patient treatment modalities.

Conclusion

Pre-treatment MRI-DWI values were unable to predict therapeutic response. However, ^{18}F-FDG PET parameters found to be more useful and were superior to DWI as a predictive parameter in patients with HNSCC.

The strength of this study is the use of an MRI-DWI parameter, which includes diffusion evaluations that were collected simultaneously during PET/MR. SUV_{max}, SUL_{peak} MTV, and TLG values, significantly predicted the clinical outcome; thus their inclusion in risk stratification may be of additional value for predicting patient treatment outcomes.

Tables

Table 5

Values are presented as the number of patients (%) unless otherwise indicated.

Characteristics	Value (%)	Characteristics	Value (%)
Number of patients	68 (100)	Initial T stage	
Mean age (year)	61±8 (46-87)	I.	5 (8)
Sex		II.	21 (31)
Men	44 (65)	III.	23 (33)
Women	24 (35)	IV.	19 (28)
Localization		Grade	
Pharynx		I.	15 (23)
Epipharynx	7 (10)	II.	35 (51)
Mesopharynx	13 (19)	III.	18 (26)
Hypopharynx	12 (18)	Presence of lymph node	
Larynx		Yes	33 (49)
Supraglottic	26 (38)	No	35 (51)
Glottic	4 (6)	Lymph node stage	
Subglottic	6 (9)	0	35 (52)
Treatment response groups		1	19 (28)
Complete Remission	36 (53)	2	9 (13)
Partial Remission	16 (24)	3	5 (7)
Stable Disease	9 (13)		
Progressive Disease	7 (10)		
Treatment response related groups			
CR	36 (53)		
non-CR	32 (47)		

Table 6

Estimated average parameters in the sub-localizations of head and neck

	Min.					**Max.**					**Mean**				
	SUV_{max} (lbm)	SUL_{peak} (SUV-lbm / Size)	TLG (SUV-lbm x cm^3)	MTV (cm^3)	ADC_{mean} $10^{-6} mm/s^2$	SUV_{max} (lbm)	SUL_{peak} (SUV-lbm / Size)	TLG (SUV-lbm x cm^3)	MTV (cm^3)	ADC_{mean} $10^{-6} mm/s^2$	SUV_{max} (lbm)	SUL_{peak} (SUV-lbm / Size)	TLG (SUV-lbm x cm^3)	MTV (cm^3)	ADC_{mean} $10^{-6} mm/s^2$
Epipharynx	2.7	2.2	4.0	2.3	640.1± 63	13.8	12.0	502.3	176.7	1212.3 ± 73	8.15	6.6	217.6	42.4	967.6± 68
Mesopharynx	3.1	2.5	3.7	2.5	622.1± 75	9.3	9.3	59.1	13.6	1107.6 ± 84	8.8	5.1	9.4	5.7	940.4± 79
Hypopharynx	3.1	2.9	25.0	8.6	613.1± 69	20.9	18.3	475.5	89.1	1200.4 ± 65	10.1	8.4	152.6	29.4	955.5± 67
Supraglottic	6.2	4.4	12.7	4.5	730.1± 70	10.8	9.2	163.4	37.0	1337.9 ± 80	8.3	6.8	80.4	15.3	910.1± 75
Glottic	5.7	4.3	15.5	4.4	690.1± 63	16.5	13.8	169.6	31.1	1095.5 ± 79	9.9	7.7	65.7	15.3	908.4± 71
Subglottic	5.7	4.1	22.5	7.0	610.3± 61	16.1	12.3	344.3	304.6	1144.6 ± 79	8.9	7.1	203.9	47.2	920.2± 70

Table 7

Correlations between DWI, and PET parameters in G1 and 2 tumors

Parameters	SUV_{max} (lbm)	SUL_{peak}(SUV-lbm / Size)	TLG (SUV-lbm x cm^3)	MTV (cm^3)	ADC_{mean}
SUV_{max} (lbm)	-	**r = 0.97** **p < 0.0001**	**r = 0.63** **p < 0.0001**	**r = 0.31** **p = 0.03**	r = -0.24 p = 0.09
SUL_{peak}(SUV-lbm / Size)		-	**r = 0.73** **p < 0.0001**	**r = 0.42** **p = 0.01**	r = -0.27 p = 0.06
TLG (SUV-lbm x cm^3)			-	**r = 0.89** **p < 0.0001**	r = -0.21 p = 0.16
MTV (cm^3)				-	r = -0.07 p = 0.59
ADC_{mean}					-

Significant correlations are highlighted in bold.

Table 8

Correlations between DWI, and PET parameters in G3 tumors

Parameters	SUV_{max} (lbm)	SUL_{peak}(SUV-lbm / Size)	TLG (SUV-lbm x cm^3)	MTV (cm^3)	ADC_{mean}
SUV_{max} (lbm)	-	**r =0.97** **p < 0.0001**	**r = 0.83** **p < 0.0001**	**r = 0.47** **p= 0.049**	r = 0.79 p = 0.75
SUL_{peak}(SUV-lbm / Size)		-	**r = 0.86** **p < 0.0001**	**r = 0.53** **p = 0.02**	r = 0.21 p = 0.93
TLG (SUV-lbm x cm^3)			-	**r = 0.83** **p < 0.0001**	r = -0.46 p = 0.86
MTV (cm^3)				-	r = -0.36 p = 0.88
ADC_{mean}					-

Significant correlations are highlighted in bold.

Figures

Figure 5

Flowchart of excluded patients

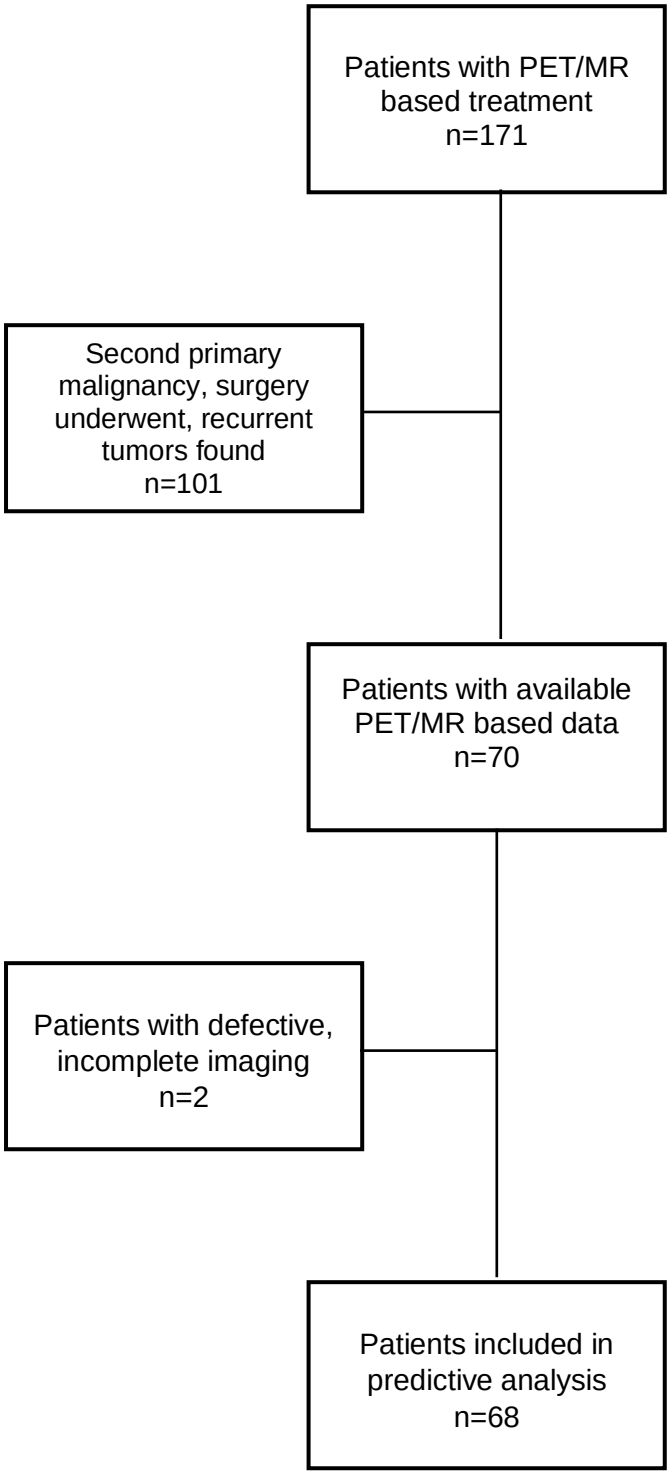

Figure 6

Axial Dixon fat suppressing (FS) T1-weighted turbo spin echo (TSE) sequence (A) used as an anatomical map. On the corresponding Apparent Diffusion Coefficient (ADC)-map (B) the area of low signal intensity, epiglottic primary tumor's (left white arrow) mean ADC (ADC_{mean}: 777.5+-42.2 10^{-6} s/mm^2) delineated (with left green ellipse), and the metastasis of largest lymph node (right white arrow) on the left side of the neck.

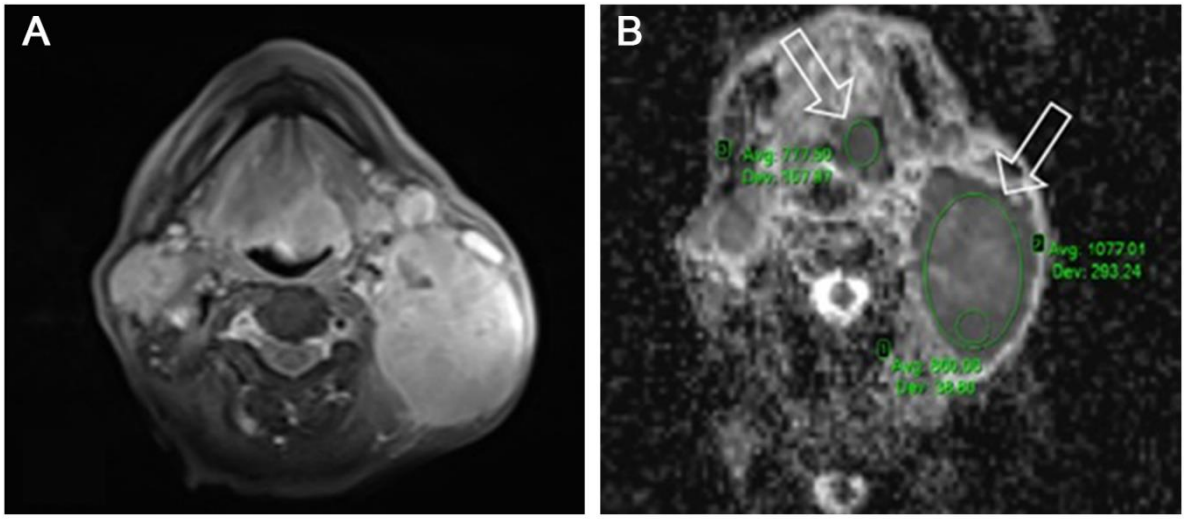

Figure 7

Complete Remission (CR): sagittal PET (A_1), coronal (B_1) and axial (C_1) PET/MR images and axial MR-Diffusion Weighted Imaging (DWI) Apparent Diffusion Coefficient (ADC) map of the tumor (D_1) show the glottic tumor spread over the supra-, and infraglottic regions, pre-treatment Maximum of Standardized Uptake Value (SUV_{max}): 14.12., Peak Lean Body Mass Corrected SUV_{max} (SUL_{peak}): 8.93, Total Lesion Glycolysis (TLG): 25.46, Metabolic Tumor Volume: 2.97 cm^3, mean ADC (ADC_{mean}): 867.22+-53.52 x 10^{-6} s/mm^2. Post-treatment sagittal PET (A_2), coronal (B_2) and axial (C_3) PET/MR images show Complete Remission (CR); without any pathologic FDG accumulation, and diffusion restriction on the observed volume. (next page)

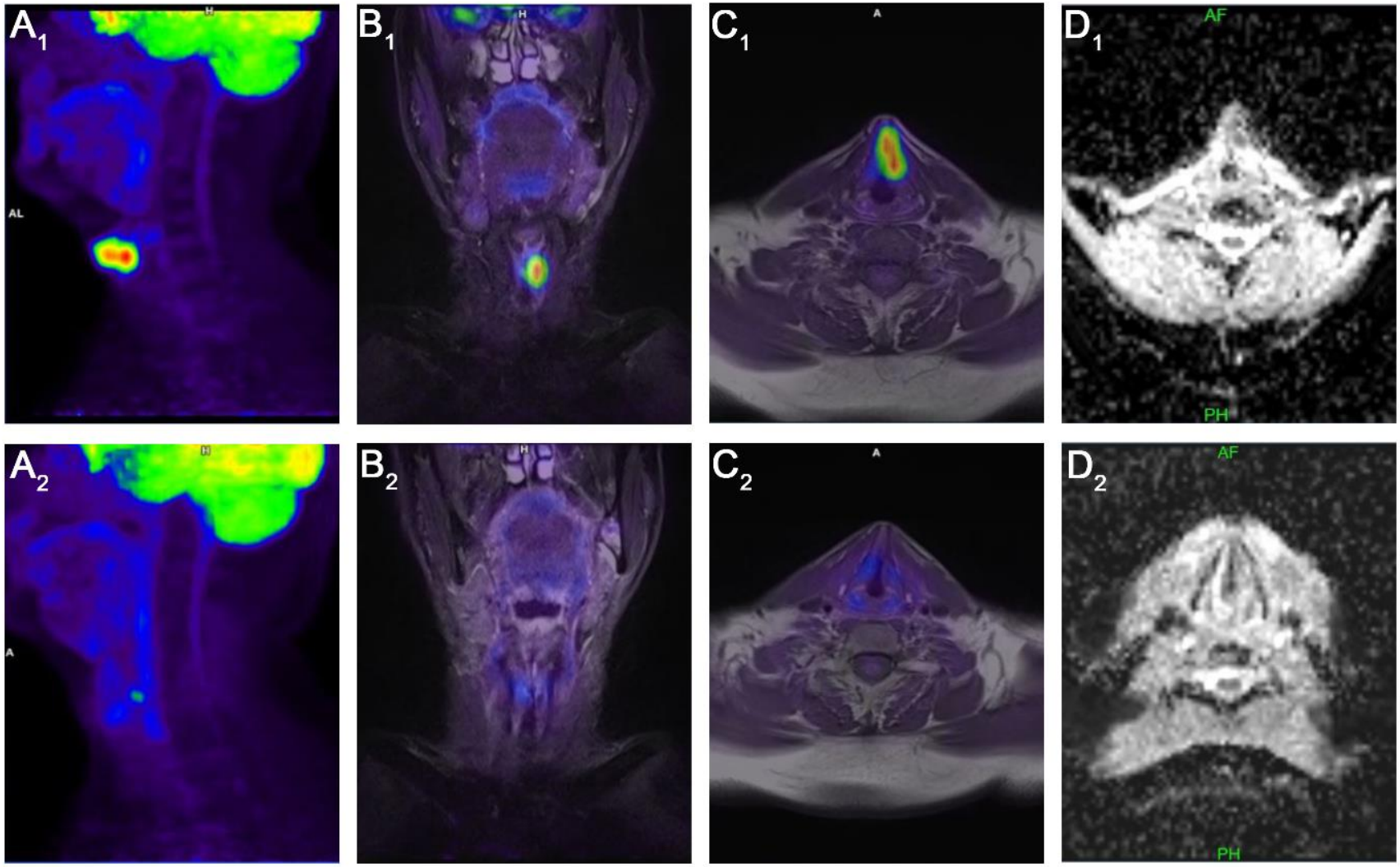
A1
B1
C1
D1
AF
PH
A2
B2
C2
D2
AF
PH

Figure 8

Correlation plots (lower triangle), histograms (diagonal), and Spearman correlation coefficients in the upper triangle are shown in the plot-matrix of pre-treatment Maximum of Standardized Uptake Value (SUV_{max}), Peak Lean Body Mass Corrected SUV_{max} (SUL_{peak}), Total Lesion Glycolysis (TLG), Metabolic Tumor Volume (MTV), Mean Apparent Diffusion Coefficient (ADC_{mean}). The significant levels are denoted by stars (*p < 0.05, ** p < 0.01, ***p < 0.001, no star: no significant).

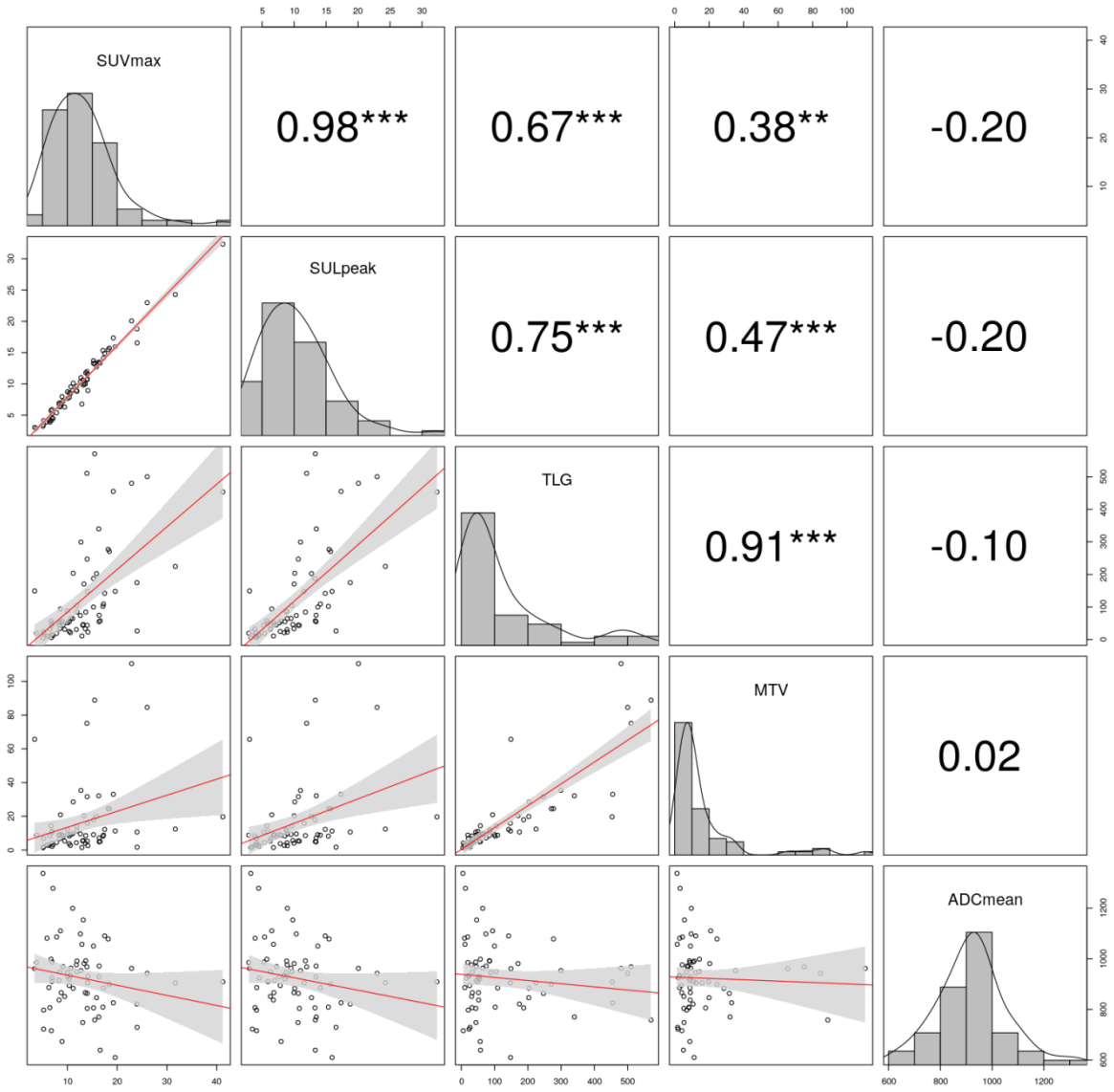

Figure 9

Boxplots show the distributions of Maximum of Standardized Uptake Value (SUV_{max}) (A), Peak Lean Body Mass Corrected SUV_{max} (SUL_{peak}) (B), Total Lesion Glycolysis (TLG) (C), Metabolic Tumor Volume (MTV) (D), Mean Apparent Diffusion Coefficient (ADC_{mean}) (E) parameters in the therapy response based subgroups, patients which achieve complete remission and non-complete remission. The p-value of the Wilcoxon rank-sum test is shown in the upper part of the plot. (next page)

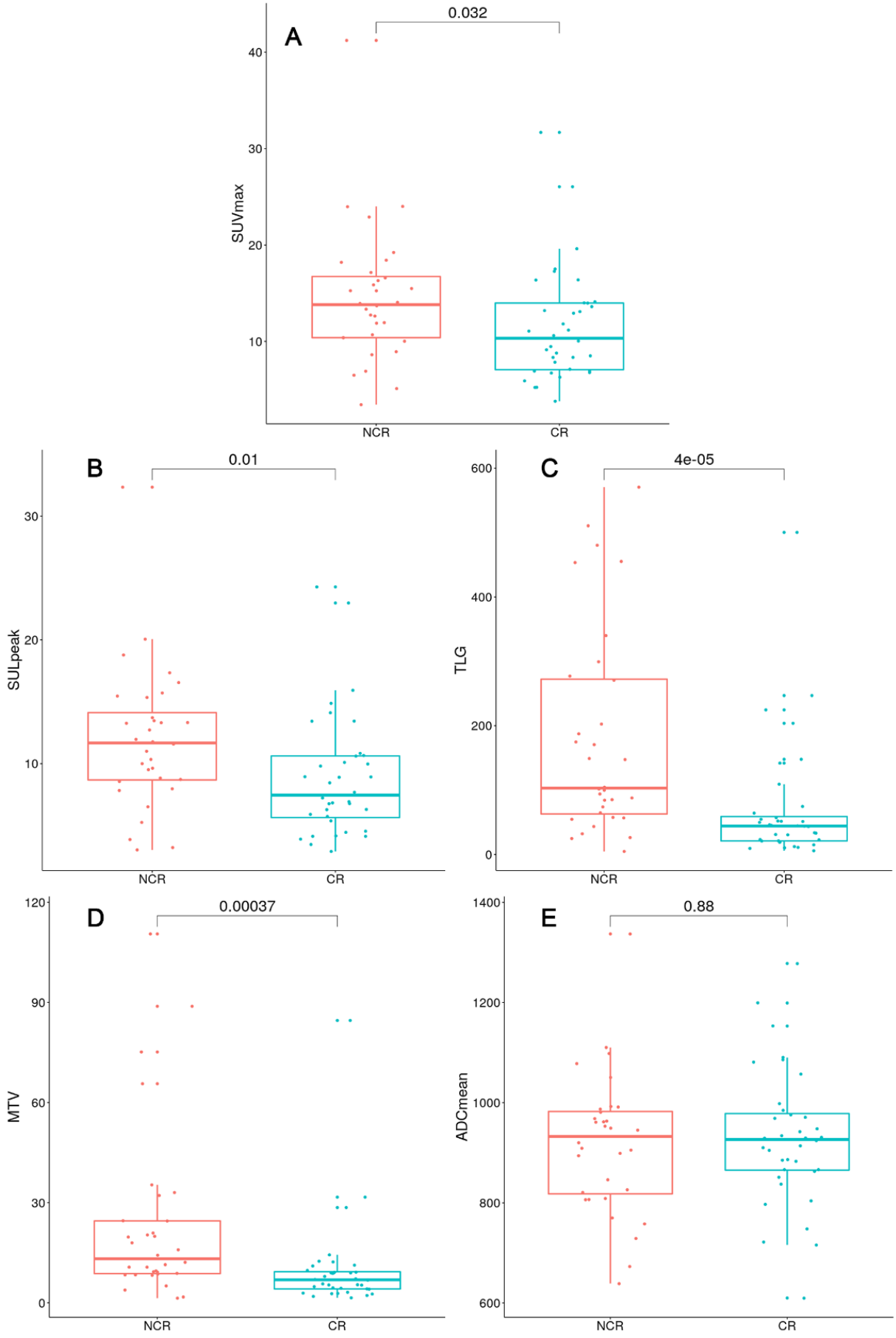
A
0.032
SUVmax
40
30
20
10
NCR
CR
B
0.01
SULpeak
30
20
10
NCR
CR
C
4e-05
TLG
600
400
200
0
NCR
CR
D
0.00037
MTV
120
90
60
30
0
NCR
CR
E
0.88
ADCmean
1400
1200
1000
800
600
NCR
CR

Summaries

Retrospective validation of coverage probability based simultaneous integrated nodal boost in locally advanced cervical cancer: a mono-institutional analysis

Introduction: To retrospectively validate Coverage probability (CovP) based simultaneous integrated nodal boost (SIB-N) concept introduced by the EMBRACE group in locally advanced cervical cancer (LACC) in terms of dosimetry, treatment verification and clinical outcome.

Material and Methods: Between 01/2016 and 09/2020 twenty-six node-positive FIGO stage ≥1B2 LACC patients (pts) were treated with external beam radiotherapy (EBRT) with concurrent chemotherapy followed by image-guided adaptive brachytherapy (IGABT). The treatment consisted of 45 Gy to the entire pelvis or pelvis + paraaortic (58% of cases) (PAO) region with 55/57.5 Gy SIB-N using volumetric arc therapy with online CBCT verification. Contouring and planning followed the EMBRACE 2 protocol. The boosted nodes were contoured on each CBCT and were assessed for coverage by the PTV-N. In patients with ≥Gr.3 non-hematologic side effect both EBRT and IGABT plans were revised, including delineation of the concerned organ on each CBCT, to allow detailed dosimetric analysis. Clinical efficacy (local failure-free- (LRFS), distant metastasis-free-(DMFS), regional failure -free (RFFS) cancer-specific-(CCS) and overall survival (OS)) was assessed by the Kaplan-Meier analysis complemented with Aalen-Johansen competing risk evaluation. Late side effects were scored using CTCAEv4.0.

Results: In total, 66 nodes (range:1-6/pts, average volume: 3.20 cm^3, r:0.8-25.3) were boosted. Dose constraints for CTV-N D98 and PTV-N D98 were achieved in 91% and 83% of the nodes, while for organs at risks they were fulfilled in ≥ 96% of the cases. During the evaluation of 650 CBCTs only two nodes in ≤3 fractions (for the same patient) were not completely covered by PTV-N. At 3 months follow-up (FUP) all cases showed regression on imaging, including 18 pts (70%) with PET/CT, where complete metabolic regression was detected in 12/18 (67%) pts. After a median FUP of 25 months (3-52) there were no nodal failure/progression either in the boosted or in the elective RT regions. The two-years actuarial/crude rates of OS/CSS/DMFS/LFFS were 90/80, 95/88, 100/92, 90/92% respectively, in alignment with the slightly worse

competing risk incidence. Eighty-nine percent of patients received ≥ 4 cycles of cisplatin with six ≥ Gr.3 hematologic side effect. One patient with PAO RT developed Grade 2 duodenal ulcer which fully recovered after conservative treatment. There was only one Gr.3 sigmoiditis with accompanying stenosis requiring elective surgical removal. In this case, both EBRT and IGABT plan respected the dose-constraints even at „worse-case" scenario for individual sigmoid locations.

Conclusion: CovP based nodal SIB boost proved to be feasible providing excellent nodal control with low rate of late toxicity confirming its place as a standard of care approach for LAPCC.

Short question: How does EMBRACE II protocol perform after implementation into clinical practice?

Pertinent findings:

- The retrospective analysis reports correlations between initial volume and clinical outcome (OS, CSS, LFFS, DMFS).
- CovP-SIB-N with daily image guidance resulted nodal control and a low rate of late toxicity.

Implications for patient care: Our experiences encourage the clinical use of CovP-SIB-N in LACC patients.

Predictive value of diffusion, glucose metabolism parameters of PET/MR in patients with head and neck squamous cell carcinoma treated with chemoradiotherapy

Purpose: This study aims to evaluate the predictive value of the pretreatment, metabolic, and diffusion parameters of a primary tumor assessed with PET/MR on patient clinical outcomes.

Materials and Methods: Retrospective evaluation was performed using PET/MR image datasets acquired using the single tracer injection dual imaging of 68 histologically proven head and neck cancer patients 4 weeks before receiving definitive chemoradiotherapy (CRT). PET/MR was performed before the CRT and 12 weeks after the CRT for response evaluation. Image data (PET and MRI-diffusion weighted imaging [DWI]) was used to specify the maximum standard uptake value, the peak lean body mass corrected, SUV_{max}, the metabolic tumor volume, the total lesion glycolysis (SUV_{max}, $SUL_{peak,}$ MTV and TLG), and the mean apparent diffusion coefficient (ADC_{mean}) of the primary tumor. Based on the results of the therapeutic response evaluation, two patient subgroups were created—one with a viable tumor, and another without. Metabolic and diffusion data, from the pretreatment PET/MR and the therapeutic response, were correlated using Spearman's correlation coefficient and Wilcoxon's test.

Results: After completing the CRT, a viable residual tumor was detected in 36/68 (53%) cases, while 32/68 (47%) patients showed complete remission. However, no significant correlation was found between the pretreatment parameter, ADC_{mean} ($p = 0.88$), and the therapeutic success. The PET parameters, SUV_{max} and SUL_{peak}, MTV, and TLG ($p = 0.032$, $p = 0.01$, $p < 0.0001$, $p = 0.0004$) were statistically significantly different between the two patient subgroups.

Conclusion: This study found that MRI-based (ADC_{mean}) data from FDG PET/MR pretreatment could not be used to predict therapeutic response, while the PET parameters SUV_{max}, SUL_{peak}, MTV, and TLG, proved to be more useful; thus their inclusion in risk stratification may also be of additional value.

Short question: How can ^{18}F-FDG PET/MR values predict the prognosis of head and neck cancer before treatment?

Pertinent finding:

- The retrospective study reveals correlations between baseline single ^{18}F-FDG tracer injection dual imaging acquisition PET-based parameters (SUV_{max}, SUL_{peak}, MTV, TLG) and MR DWI (ADC_{mean})-based parameter, and therapy response, after treatment (CR, NCR).

Implications for patient care: Clinicians should measure and integrate the suggested parameters (SUV_{max}, SUL_{peak} MTV, TLG) with PET/MR to provide the most accurate therapy for the patient.

Summary of novel findings

Retrospective validation of coverage probability based simultaneous integrated nodal boost in locally advanced cervical cancer: a mono-institutional analysis

With daily imaging guidance, CovP-SIB-N achieved nodal control and a low risk of late toxicity.

Correlations between initial volume and clinical outcome are reported in the retrospective analysis (OS, CSS, LFFS, DMFS).

Predictive value of diffusion, glucose metabolism parameters of PET/MR in patients with head and neck squamous cell carcinoma treated with chemoradiotherapy

The retrospective investigation found a significant between baseline single ^{18}F-FDG tracer injection dual imaging acquisition PET-based parameters (SUV_{max}, SUL_{peak}, MTV, TLG) and MR DWI (ADC_{mean})-based parameters.

There are correlations occurred in terms of therapy response following treatment (CR, NCR) and PET parameters.

Acknowledgement

I would like to sincerely thank with the greatest thankfulness for my supervisors, Dr. habil. Árpád Kovács and Dr. habil. Ferenc Lakosi for advice and guidance during my doctoral research.

I would also like to sincerely thank to, Prof. Dr. József Bódis, the Head of Doctoral School and to Prof. Dr. Endre Sulyok, Secretary of the Doctoral School of Health Sciences supported from the beginning of my research work.

I am grateful to the leaders of the Somogy County Kaposi Mór Teaching Hospital, Dr. József Baka Center, and Medicopus Non-Profit Ltd.: especially Dr. Mariann Moizs PhD., Prof. Dr. Imre Repa and Dr. Zoltán Tóth for providing the opportunity for performing my scientific work beside my professional duties.

I would like to express my gratitude to Dr. Ákos Gulybán and Dr. Miklós Emri for providing the finest statistical analysis and for their great cooperation.

I am also grateful to Institute of Diagnostics, Faculty of Health Sciences, University of Pécs for support, and to everyone who contributed to the Somogy County Kaposi Mór Teaching Hospital, Dr. József Baka Center, Department of Oncoradiology.

Last but not least, I am sincerely thankful for my family - especially Brigitta - my parents, my sister and my brother. They provided a balanced and peaceful family background for my doctoral activity. I am grateful to them for their time and patience.

Published journal papers within the topic

Freihat O, Zoltán T, Pinter T, **Kedves A**, Sipos D, Repa I, Kovács Á, Zsolt C. Correlation between Tissue Cellularity and Metabolism Represented by Diffusion-Weighted Imaging (DWI) and 18F-FDG PET/MRI in Head and Neck Cancer (HNC). Cancers. 2022; 14(3):847. https://doi.org/10.3390/cancers14030847 **Q1 6.16 IF**

Kedves A, Gulyban A, Glavak C, et al. Retrospective validation of coverage probability based simultaneous integrated nodal boost in locally advanced cervical cancer: a mono-institutional analysis . *Acta Oncol*. 2021;1-4. doi:10.1080/0284186X.2021.1971293 **Q1, 4.0 IF$_{2020}$.**

Kedves A, Tóth Z, Emri M, Fábián K, Sipos D, Freihat O, Tollár J, Cselik Z, Lakosi F, Bajzik G, Repa I and Kovács Á (2020) Predictive Value of Diffusion, Glucose Metabolism Parameters of PET/MR in Patients With Head and Neck Squamous Cell Carcinoma Treated With Chemoradiotherapy. Front. Oncol. 10:1484. doi: 10.3389/fonc.2020.01484. **Q1, 6.23 IF$_{2020}$.**

Freihat, O., Pinter, T., **Kedves, A**. et al. Diffusion-Weighted Imaging (DWI) derived from PET/MRI for lymph node assessment in patients with Head and Neck Squamous Cell Carcinoma (HNSCC). Cancer Imaging 20, 56 (2020). https://doi.org/10.1186/s40644-020-00334-x. **Q1, 2.3 IF**.

Freihat O, Tóth Z, Pintér T, **Kedves A**, Sipos D, Cselik Z, Lippai N, Repa I, Kovács Á. Pre-treatment PET/MRI based FDG and DWI imaging parameters for predicting HPV status and tumor response to chemoradiotherapy in primary oropharyngeal squamous cell carcinoma (OPSCC). Oral Oncol. 2021 Feb 25;116:105239. doi: 10.1016/j.oraloncology.2021.105239. PMID: 33640578. **Q1, 3.99 IF**.

Zsolt Cselik MD, PhD, Zoltán Tóth MD, **András Kedves** MSc, Dávid Sipos MSc, Omar Freihat MSc, Tímea Vecsera , Gábor Lukács MD, PhD, Miklós Emri MD, PhD, Gábor Bajzik MD, PhD, Janaki Hadjiev MD, PhD, Imre Repa MD, PhD, Mariann Moizs MD, PhD, Árpád Kovács Predictive value of PET/CT based metabolic information in the modern 3D based radiotherapy treatment of head and neck cancerpatients – single institute study. MD, PhD. Hellenic Journal of Nuclear Medicine **Q3, 1.0 IF**.

Omar FREIHAT, Zoltán TÓTH, Tamas PINTER, **András KEDVES** et al. Association Between Diffusion Weighted-Imaging (DWI) and Simultaneous 18F-FDG-PET/MRI Parameters with a Comparison of their Diagnostical Role in Head and Neck Squamous Cell Carcinoma (HNSCC), EJNMMI RES. 13 July 2020, doi: 10.21203/rs.3.rs-40989/v1, **Q1, 3.1 IF**.

Published journal papers related to topic:

Tollár, József ; Nagy, Ferenc ; Csutorás, Bence ; Prontvai, Nándor ; Nagy, Zsófia ; Török, Katalin ; Blényesi, Eszter ; Vajda, Zsolt ; Farkas, Dóra ; Tóth, Béla E., **András, Kedves** et al. High frequency and intensity rehabilitation in 641 sub-acute ischemic stroke patients ARCHIVES OF PHYSICAL MEDICINE AND REHABILITATION 102 : 1 pp. 9-18. , 10 p. (2021) **Q1, 3.9 IF.**

Kovács, Árpád ; Sipos, Dávid ; Lukács, Gábor ; Tóth, Zoltán ; Vecsera, Tímea ; **Kedves, András** ; Cselik, Zsolt ; Pandur, Attila András ; Bajzik, Gábor ; Repa, Imre et al. A PET/CT szerepe a sugárkezelésre kerülő betegek N és M klinikai stagingjében, a terápia meghatározásában: Intézeti tapasztalatok ORVOSI HETILAP 159 : 39 pp. 1593-1601. , 9 p. (2018) **Q3, 0,6 IF**.

Presentations, published abstracts, posters related to topic:

András, Kedves ; Metin, Akay ; Yasemine, Akay ; Ting, Chen ; Katalin, Kisiván ; Csaba, Glavák ; Ádám, Schiffer ; Aba, Lőrinc ; András, Szőke ; Árpád, Kovács et al. PREDICTIVE VALUE OF DIFFUSION PARAMETERS USING ARTIFICIALINTELLIGENCE IN LOW-AND INTERMEDIATE-RISK PROSTATE CANCER PATIENTS TREATED WITH STEREOTACTIC ABLATIVE RADIOTHERAPY Abstract Book of the 1st International Conference of Biomedical Engineering and Innovation : University of Pécs 24-26. October 2022 Pécs, Magyarország : PTE 59 p. p. 23 (2022)

András Kedves, Katalin Kisiván, Csaba Glavák, Aba Lőrincz, Árpád Kovács, Ferenc Lakosi Assessment of Pretreatment Diffusion Parameters in Low-and Intermediate-risk Prostate Cancer Patients Treated with Stereotactic Ablative Radiotherapy EUROPEAN JOURNAL OF NUCLEAR MEDICINE AND MOLECULAR IMAGING Barcelona, Spanyolország: ur J Nucl Med Mol Imaging 49 (Suppl 1), 113-113 (EANM) (2022)

Lakosi, Ferenc ; **Kedves, András** ; Gulybán, Ákos ; Toller, Gábor ; Völgyi, Zoltán ; Faour, Amer ; Bálint, András ; Petrási, Bernadett ; Glavák, Csaba Céltérfogat lefedettség valószínűségen („Coverage probability based") alapuló szimultán integrált nyirokcsomó boost technika lokálisan előrehaladott méhnyakrák esetén: 2 éves eredmények MAGYAR ONKOLÓGIA 66 : 1 pp. 81-82. , 2 p. (2022)

A., Kedves ; C., Glavak ; G., Antal ; G., Toller ; Z., Volgyi ; A., Faour ; B., Petrasi ; A., Gulyban ; F., Lakosi Retrospective validation of coverage probability based SIB-N in LACC a mono-institunional analysis RADIOTHERAPY AND ONCOLOGY 161 : Suppl 1 pp. S647-S648. (2021)

A., Kedves ; M., Emri ; K., Fabian ; D., Sipos ; O., Freihat ; J., Tollar ; Z., Cselik ; G., Bajzik ; I., Repa ; A., Kovacs et al. Predictive value of multiparametric PET/MR in patients with head and neck squamous cell carcinoma treated with chemoradiotherapy EUROPEAN JOURNAL OF NUCLEAR MEDICINE AND MOLECULAR IMAGING 47 : Suppl 1 pp. S310-S310. Paper: OP-613 (2020)

Kedves, A. ; Kövesdi, O ; Tóth, Z. ; Sipos., D. ; O., Freihat ; Cselik, Z. ; Moizs, M. ; Kovacs, A. ; Repa, I. Predictive value of 18F-FDG PET/MR at head and neck cancer

patient treated with chemoradiotherapy – methodology case study In: European Congress of Radiology (ECR 2020) Vienna, Ausztria : European Society of Radiology (2020)

Rajnics, Péter ; Egyed, Miklós ; Tóth, Zoltán ; **Kedves, András** ; Kollár, Balázs ; Karádi, Éva ; Kellner, Ádám ; Ercsei, Ibolya ; Moizs, Mariann ; Repa, Imre PET/CT vizsgálatok szerepe myelomás betegeinknél (2020) Előadás, VIII. Miskolci Myeloma Konferencia, Lillafüred, 2020. február 28–29.,

A., Kedves ; Z., Tóth ; T., Pintér ; B., Sánta ; Z., Cselik ; V., Koczka ; D., Sipos ; F., Omar ; G., Bajzik ; J., Hadijev et al. 18F-FDG PET/MR multiparametric measurement of head and neck cancer patients underwent modern 3D based radiotherapy - preliminary results In: Andrea, Santos; MarieClaire, Attard; Marius, Mada; Barbora, Trnena (szerk.) Annual Congress of the European Association of Nuclear Medicine : Technologist abstract book Barcelona, Spanyolország : European Association of Nuclear Medicine (EANM) (2019)

A., Kedves ; Z., Tóth ; T., Pintér ; B., Sánta ; Z., Cselik ; V., Koczka ; D., Sipos ; F., Omar ; G., Bajzik ; J., Hadijev et al. 18F-FDG PET/MR multiparametric measurement of head and neck cancer patients underwent modern 3D based radiotherapy - preliminary results EUROPEAN JOURNAL OF NUCLEAR MEDICINE AND MOLECULAR IMAGING 46 : Suppl. 1 pp. S886-S887. Paper: TEPS-80 , 1 p. (2019)

Kedves, A ; Vecsera, T ; Sipos, D ; Emri, M ; Tóth, Z ; Koczka, V ; Kelemen, K ; Repa, I ; Kovacs, A 18F-FDG PET/CT based target volume definition in the modern 3D Radiotherapy In: Sn (szerk.) ECR 2019 Bécs, Ausztria : European Society of Radiology (2019)

Kedves, A ; Tóth, Z ; Emri, M ; Sipos, D ; Koczka, V ; Repa, I ; Kovács, Á Predictive value of 18F-FDG PET/CT information in the modern 3D-based radiotherapy treatment of head and neck cancer patients INSIGHTS INTO IMAGING 10 : Suppl. 1 Paper: B-0882 (2019)

Kedves, A. ; Tóth, Z. ; Emri, M. ; Sipos, D. ; Repa, I. ; Kovács, Á. Biológiai nyirokcsomó céltérfogat meghatározás [18]F-FDG PET/CT alapú képanyagon 3D modern besugárzásban részesülő betegeknél In: MONT XXI. kongresszus 2019 : Absztraktgyűjtemény (2019)

Kedves, András ; Tóth, Zoltán ; Emri, Miklós ; Sipos, Dávid ; Repa, Imre ; Kovács, Árpád Assessment of biological target volume nodal based on [18]F-FDG PET/CT at patients treated with 3d modern radiotherapy In: Klavdija, ČUČEK TRIFKOVIČ; Ines, MLAKAR 11. Študentska konferenca s področja zdravstvenih ved z mednarodno udeležbo : Raziskovanje študentov zdravstvenih ved prispeva k zdravju in razvoju sodobne družbe Maribor, Szlovénia : Univerzitetna založba Univerze v Mariboru (2019)

Zoltán, Tóth ; Gábor, Lukács ; **András, Kedves** ; Miklós, Emri ; Zsolt, Cselik ; Gábor, Toller ; Éva, Ferenczy ; Ferenc, Lakosi ; Janaki, Hadjiev ; Imre, Repa et al. PREDICTIVE ROLE OF FDG PET/CT IN HEAD AND NECK CANCER TREATED WITH RADIOTHERAPY — PRELIMINARY RESULTS NUCLEAR MEDICINE REVIEW: CENTRAL AND EASTERN EUROPE 20 : 2 Paper: T3-2 , 1 p. (2017)

Awards, scholarships related to the topic

Campus Mundi Scholarship - Biomedical Engineer Intern - Scholar in the Department of Biomedical Engineering (programme: “artificial intelligence (AI) in medical imaging”) - University of Houston, Houston, Texas, USA
Issued by Tempus Public Foundation · Jul 2022

Minister of Education awards the Fellowship granted by the Republic (“Köztársasági ösztöndíj”)
Issued by Ministry of Human Capacities · Sep 2022

New National Excellence Program
Issued by National Research Development and Innovation Office · Aug 2022

MEDISO-Award
Issued by George de Hevesy Hungarian Society of Nuclear Medicine · May 2022

New National Excellence Program of the Ministry of Human Capacities and the Ministry for Innovation and Technology
Issued by Ministry of Human Capacities · Aug 2020

Shape Your Skills Award European Congress of Radiology 2020
Issued by European Society of Radiology · Dec 2019

Best Paper Abstract Award European Congress of Radiology (ECR) 2019
Issued by European Society of Radiology (ESR), Vienna, Austria · Mar 2019

National Conference of Scientific Students' Association ("OTDK") 1st place
Issued by Council of National Scientific Students' Association · May 2017

Appendix
Appendix 1

The Revised Federation of Gynecology and Obstetrics (FIGO) Staging System

Source: https://doi.org/10.1148/rg.326125519

Stage	Description
0	Tumor confined to the surface layer (the cell lining) of the cervix; also called carcinoma in situ
I	Extension deeper into the cervix with no spread beyond (extension to the corpus is disregarded)
IA	Invasive carcinoma; may only be diagnosed at microscopy
IA1	Stromal invasion 3.0 mm deep and extension 7.0 mm
IA2	Stromal invasion >3.0 mm and 5.0 mm with extension ≤7.0 mm
IB	Clinically visible lesions limited to the cervix uteri or preclinical cancers higher than stage IA
IB1	Clinically visible lesion 4.0 cm in greatest dimension
IB2	Clinically visible lesion >4.0 cm in greatest dimension
II	Cervical carcinoma extends beyond the uterus but not to the pelvic wall or the lower one-third of the vagina
IIA	No parametrial invasion
IIA1	Clinically visible lesion 4.0 cm in greatest dimension
IIA2	Clinically visible lesion >4.0 cm in greatest dimension
IIB	With obvious parametrial invasion
III	Extension to the pelvic wall, involvement of lower one-third of the vagina, or hydronephrosis or nonfunctioning kidney
IIIA	Involvement of lower one-third of the vagina with no extension to the pelvic wall
IIIB	Extension to the pelvic wall, hydronephrosis, or nonfunctioning kidney
IV	Extension beyond the true pelvis or involvement of the bladder or rectal mucosa (biopsy proved); bullous edema does not convey stage IV disease
IVA	Spread to adjacent organs
IVB	Spread to distant organs

Appendix 2

2014 International Society of Urological Pathology (ISUP) Gleason score and Gleason grade groups 15

Source: [10.1097/PAS.0000000000000530](10.1097/PAS.0000000000000530)

Gleason Grade group	Score	Definition
1	3+3=6	Only individual discrete well-formed glands
2	3+4=7	Predominantly well-formed glands with a lesser component of poorly/fused/cribriform glands
3	4+3=7	Predominantly poorly formed/fused/cribriform glands with a lesser component of well-formed glands
4	5+3, 3+5, 4+4 (Gleason score 8)	Only poorly formed/fused/cribriform glands(>95%) or Predominantly well-formed glands and lesser component lacking glands or Predomi-

Appendix 3

Interfractional variability of sigmoid bowel (*white*: planning CT, *magenta*: 1-25th fractions) in patient with Gr.3 GI event treated by CovP-SIB-N for 3 nodal targets.

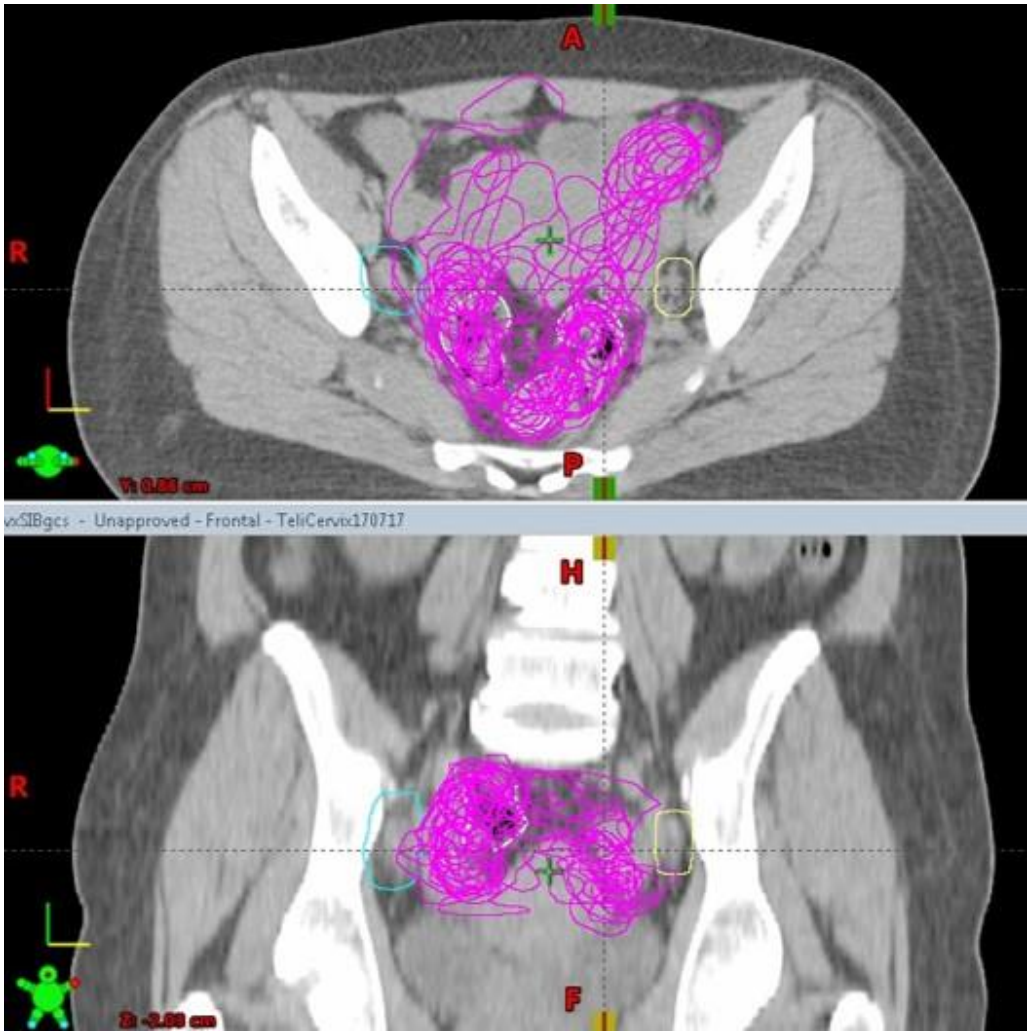

Bibliography

[1] Parkin DM, Pisani P, Ferlay J. Global cancer statistics. CA Cancer J Clin. 1999;49(1):33-1. doi:10.3322/canjclin.49.1.33

[2] Arbyn M, Castellsagué X, de Sanjosé S, et al. Worldwide burden of cervical cancer in 2008. Ann Oncol. 2011;22(12):2675-2686. doi:10.1093/annonc/mdr015

[3] Ottó S, Kásler M. A hazai és nemzetközi daganatos halálozási és megbetegedési mutatók alakulása. A népegészségügyi programok jellegzetességei és várható eredményei [Trends in cancer mortality and morbidity in Hungarian and international statistics. Characteristics and potential outcome of public health screening programs]. Magy Onkol. 2005;49(2):99-107.

[4] http://stat.nrr.hu

[5] The 1988 Bethesda System for reporting cervical/vaginal cytological diagnoses. National Cancer Institute Workshop. JAMA. 1989;262(7):931-934.

[6] Sung H, Ferlay J, Siegel RL, et al. Global Cancer Statistics 2020: GLOBOCAN Estimates of Incidence and Mortality Worldwide for 36 Cancers in 185 Countries. CA Cancer J Clin. 2021;71(3):209-249. doi:10.3322/caac.21660

[7] Partin AW, Kattan MW, Subong EN, et al. Combination of prostate-specific antigen, clinical stage, and Gleason score to predict pathological stage of localized prostate cancer. A multi-institutional update [published correction appears in JAMA 1997 Jul 9;278(2):118]. *JAMA*. 1997;277(18):1445-1451.

[8] Epstein JI, Egevad L, Amin MB, et al. The 2014 International Society of Urological Pathology (ISUP) Consensus Conference on Gleason Grading of Prostatic Carcinoma: Definition of Grading Patterns and Proposal for a New Grading System. Am J Surg Pathol. 2016;40(2):244-252. doi:10.1097/PAS.0000000000000530

[9] D'Amico AV, Whittington R, Malkowicz SB, et al. Biochemical outcome after radical prostatectomy, external beam radiation therapy, or interstitial radiation therapy for clinically localized prostate cancer. JAMA. 1998;280(11):969-974. doi:10.1001/jama.280.11.969

[10] Buyyounouski MK, Choyke PL, McKenney JK, et al. Prostate cancer - major changes in the American Joint Committee on Cancer eighth edition cancer staging manual. CA Cancer J Clin. 2017;67(3):245-253. doi:10.3322/caac.21391

[11] Höckel M. Neue Konzepte für die operative Therapie des Zervixkarzinoms [New concepts for surgical therapy of cervical carcinoma]. Pathologe. 2005;26(4):276-282. doi:10.1007/s00292-005-0762-5

[12] Kedves A, Gulyban A, Glavak C, et al. Retrospective validation of coverage probability based simultaneous integrated nodal boost in locally advanced cervical cancer: a mono-institutional analysis . *Acta Oncol*. 2021;1-4. doi:10.1080/0284186X.2021.1971293

[13] Hashibe M, Hunt J, Wei M, Buys S, Gren L, Lee YC. Tobacco, alcohol, body mass index, physical activity, and the risk of head and neck cancer in the prostate, lung, colorectal, and ovarian (PLCO) cohort. Head Neck. 2013;35(7):914-922. doi:10.1002/hed.23052

[14] Global Burden of Disease Cancer Collaboration, Fitzmaurice C, Abate D, et al. Global, Regional, and National Cancer Incidence, Mortality, Years of Life Lost, Years Lived With Disability, and Disability-Adjusted Life-Years for 29 Cancer Groups, 1990 to 2017: A Systematic Analysis for the Global Burden of Disease Study [published correction appears in JAMA Oncol. 2020 Mar 1;6(3):444] [published correction appears in JAMA Oncol. 2020 May 1;6(5):789] [published correction appears in JAMA Oncol. 2021 Mar 1;7(3):466]. JAMA Oncol. 2019;5(12):1749-1768. doi:10.1001/jamaoncol.2019.2996

[15] Aupérin A. Epidemiology of head and neck cancers: an update. Curr Opin Oncol. 2020;32(3):178-186. doi:10.1097/CCO.0000000000000629

[16] Available at: https://Gco.Iarc.Fr/Today/Data/Factsheets/Populations/348-Hungary-Fact-Sheets.Pdf, 004, 2018–2019.

[17] OECD/European Observatory on Health Systems and Policies (2017), Hungary: Country Health Profile 2017, State of Health in the EU, OECD Publishing,

Paris/European Observatory on Health Systems and Policies, Brussels, https://doi.org/10.1787/9789264283411-en.

[18] Tamás, J. (2018). PhD Thesis Molecular examination of the microenvironment of head and neck tumors. 0–21

[19] Blot WJ, McLaughlin JK, Winn DM, et al. Smoking and drinking in relation to oral and pharyngeal cancer. Cancer Res. 1988;48(11):3282-3287.

[20] Cruz I, Van den Brule AJ, Steenbergen RD, et al. Prevalence of Epstein-Barr virus in oral squamous cell carcinomas, premalignant lesions and normal mucosa--a study using the polymerase chain reaction. Oral Oncol. 1997;33(3):182-188. doi:10.1016/s0964-1955(96)00054-1

[21] Larsson PA, Edström S, Westin T, Nordkvist A, Hirsch JM, Vahlne A. Reactivity against herpes simplex virus in patients with head and neck cancer. Int J Cancer. 1991;49(1):14-18. doi:10.1002/ijc.2910490104

[22] Deeken JF, Tjen-A-Looi A, Rudek MA, et al. The rising challenge of non-AIDS-defining cancers in HIV-infected patients. *Clin Infect Dis*. 2012;55(9):1228-1235. doi:10.1093/cid/cis613

[23] Guha N, Warnakulasuriya S, Vlaanderen J, Straif K. Betel quid chewing and the risk of oral and oropharyngeal cancers: a meta-analysis with implications for cancer control. *Int J Cancer*. 2014;135(6):1433-1443. doi:10.1002/ijc.28643

[24] Hashim D, Sartori S, Brennan P, et al. The role of oral hygiene in head and neck cancer: results from International Head and Neck Cancer Epidemiology (INHANCE) consortium. Ann Oncol. 2016;27(8):1619-1625. doi:10.1093/annonc/mdw224

[25] Hashim D, Sartori S, Brennan P, et al. The role of oral hygiene in head and neck cancer: results from International Head and Neck Cancer Epidemiology (INHANCE) consortium. Ann Oncol. 2016;27(8):1619-1625. doi:10.1093/annonc/mdw224

[26] Freihat O, Zoltán T, Pinter T, Kedves A, Sipos D, Repa I, Kovács Á, Zsolt C. Correlation between Tissue Cellularity and Metabolism Represented by Diffusion-Weighted Imaging (DWI) and 18F-FDG PET/MRI in Head and Neck Cancer (HNC). Cancers. 2022; 14(3):847. https://doi.org/10.3390/cancers14030847

[27] Kedves A, Tóth Z, Emri M, Fábián K, Sipos D, Freihat O, Tollár J, Cselik Z, Lakosi F, Bajzik G, Repa I and Kovács Á (2020) Predictive Value of Diffusion, Glucose Metabolism Parameters of PET/MR in Patients With Head and Neck Squamous Cell Carcinoma Treated With Chemoradiotherapy. Front. Oncol. 10:1484. doi: 10.3389/fonc.2020.01484.

[28] Freihat, O., Pinter, T., Kedves, A. et al. Diffusion-Weighted Imaging (DWI) derived from PET/MRI for lymph node assessment in patients with Head and Neck Squamous Cell Carcinoma (HNSCC). Cancer Imaging 20, 56 (2020). https://doi.org/10.1186/s40644-020-00334-x.

[29] Freihat O, Tóth Z, Pintér T, et al. Pre-treatment PET/MRI based FDG and DWI imaging parameters for predicting HPV status and tumor response to chemoradiotherapy in primary oropharyngeal squamous cell carcinoma (OPSCC). Oral Oncol. 2021;116:105239. doi:10.1016/j.oraloncology.2021.105239

[30] Cselik Z, Tóth Z, Kedves A, et al. Predictive value of PET/CT based metabolic information in the modern 3D based radiotherapy treatment of head and neck can-cer patients - single institute study. Hell J Nucl Med. 2020;23(3):290-295. doi:10.1967/s002449912207

[31] Freihat O, Zoltán T, Pinter T, et al. Correlation between Tissue Cellularity and Metabolism Represented by Diffusion-Weighted Imaging (DWI) and 18F-FDG PET/MRI in Head and Neck Cancer (HNC). Cancers (Basel). 2022;14(3):847. Published 2022 Feb 8. doi:10.3390/cancers14030847

[32] Pötter R, Georg P, Dimopoulos JC, et al. Clinical outcome of protocol based image (MRI) guided adaptive brachytherapy combined with 3D conformal radiotherapy with or without chemotherapy in patients with locally advanced cervical cancer. Radiother Oncol. 2011;100(1):116-123. doi:10.1016/j.radonc.2011.07.012

[33] Lindegaard JC, Fokdal LU, Nielsen SK, Juul-Christensen J, Tanderup K. MRI-guided adaptive radiotherapy in locally advanced cervical cancer from a Nordic perspective. Acta Oncol. 2013;52(7):1510-1519. doi:10.3109/0284186X.2013.818253

[34] Nomden CN, de Leeuw AA, Roesink JM, et al. Clinical outcome and dosimetric parameters of chemo-radiation including MRI guided adaptive brachytherapy with

tandem-ovoid applicators for cervical cancer patients: a single institution experience. Radiother Oncol. 2013;107(1):69-74. doi:10.1016/j.radonc.2013.04.006

[35] Castelnau-Marchand P, Chargari C, Maroun P, et al. Clinical outcomes of definitive chemoradiation followed by intracavitary pulsed-dose rate image-guided adaptive brachytherapy in locally advanced cervical cancer. Gynecol Oncol. 2015;139(2):288-294. doi:10.1016/j.ygyno.2015.09.008

[36] Castelnau-Marchand P, Chargari C, Maroun P, et al. Clinical outcomes of definitive chemoradiation followed by intracavitary pulsed-dose rate image-guided adaptive brachytherapy in locally advanced cervical cancer. Gynecol Oncol. 2015;139(2):288-294. doi:10.1016/j.ygyno.2015.09.008

[37] Gill BS, Kim H, Houser CJ, et al. MRI-guided high-dose-rate intracavitary brachytherapy for treatment of cervical cancer: the University of Pittsburgh experience. Int J Radiat Oncol Biol Phys. 2015;91(3):540-547. doi:10.1016/j.ijrobp.2014.10.053

[38] Lakosi F, de Cuypere M, Viet Nguyen P, et al. Clinical efficacy and toxicity of radio-chemotherapy and magnetic resonance imaging-guided brachytherapy for locally advanced cervical cancer patients: A mono-institutional experience. Acta Oncol. 2015;54(9):1558-1566. doi:10.3109/0284186X.2015.1062542

[39] Ribeiro I, Janssen H, De Brabandere M, et al. Long term experience with 3D image guided brachytherapy and clinical outcome in cervical cancer patients. Radiother Oncol. 2016;120(3):447-454. doi:10.1016/j.radonc.2016.04.016

[40] Sturdza A, Pötter R, Fokdal LU, et al. Image guided brachytherapy in locally advanced cervical cancer: Improved pelvic control and survival in RetroEMBRACE, a multicenter cohort study. Radiother Oncol. 2016;120(3):428-433. doi:10.1016/j.radonc.2016.03.011

[41] Pötter R, Tanderup K, Schmid MP, et al. MRI-guided adaptive brachytherapy in locally advanced cervical cancer (EMBRACE-I): a multicentre prospective cohort study. Lancet Oncol. 2021;22(4):538-547. doi:10.1016/S1470-2045(20)30753-1

[42] Jürgenliemk-Schulz IM, Beriwal S, de Leeuw AAC, et al. Management of Nodal Disease in Advanced Cervical Cancer. Semin Radiat Oncol. 2019;29(2):158-165. doi:10.1016/j.semradonc.2018.11.002

[43] Nomden CN, Pötter R, de Leeuw AAC, et al. Nodal failure after chemo-radiation and MRI guided brachytherapy in cervical cancer: Patterns of failure in the EMBRACE study cohort. Radiother Oncol. 2019;134:185-190. doi:10.1016/j.radonc.2019.02.007

[44] Jayatilakebanda I, Tsang YM, Hoskin P. High dose simultaneous integrated boost for node positive cervical cancer [published correction appears in Radiat Oncol. 2021 Aug 18;16(1):156]. Radiat Oncol. 2021;16(1):92. Published 2021 May 17. doi:10.1186/s13014-021-01818-1

[45] Ramlov A, Assenholt MS, Jensen MF, et al. Clinical implementation of coverage probability planning for nodal boosting in locally advanced cervical cancer. Radiother Oncol. 2017;123(1):158-163. doi:10.1016/j.radonc.2017.01.015

[46] Lindegaard JC, Assenholt M, Ramlov A, Fokdal LU, Alber M, Tanderup K. Early clinical outcome of coverage probability based treatment planning for simultaneous integrated boost of nodes in locally advanced cervical cancer. Acta Oncol. 2017;56(11):1479-1486. doi:10.1080/0284186X.2017.1349335

[47] Pötter R, Tanderup K, Kirisits C, et al. The EMBRACE II study: The outcome and prospect of two decades of evolution within the GEC-ESTRO GYN working group and the EMBRACE studies. Clin Transl Radiat Oncol. 2018;9:48-60. Published 2018 Jan 11. doi:10.1016/j.ctro.2018.01.001

[48] Berger T, Fokdal LU, Assenholt MS, et al. Robustness of elective lymph node target coverage with shrinking Planning Target Volume margins in external beam radiotherapy of locally advanced cervical cancer. Phys Imaging Radiat Oncol. 2019;11:9-15. Published 2019 Jun 26. doi:10.1016/j.phro.2019.06.002

[49] ICRU Report 89 Prescribing, Recording and Reporting Brachytherapy for Cancer of the Cervix: International Commision of Radiation Unit and Measurement, vol. 13, Oxford University Press, Oxford, UK (2013), pp. 133-141

[50] Edwards JK, Hester LL, Gokhale M, Lesko CR. Methodologic Issues When Estimating Risks in Pharmacoepidemiology. Curr Epidemiol Rep. 2016;3(4):285-296. doi:10.1007/s40471-016-0089-1

[51] Ramlov A, Kroon PS, Jürgenliemk-Schulz IM, et al. Impact of radiation dose and standardized uptake value of (18)FDG PET on nodal control in locally advanced cervical cancer. Acta Oncol. 2015;54(9):1567-1573. doi:10.3109/0284186X.2015.1061693

[52] Bacorro W, Dumas I, Escande A, et al. Dose-volume effects in pathologic lymph nodes in locally advanced cervical cancer. Gynecol Oncol. 2018;148(3):461-467. doi:10.1016/j.ygyno.2017.12.028

[53] Argiris A, Karamouzis MV, Raben D, Ferris RL. Head and neck cancer. Lancet. 2008;371(9625):1695-1709. doi:10.1016/S0140-6736(08)60728-X

[54] Avallone A, Aloj L, Pecori B, et al. 18F-FDG PET/CT Is an Early Predictor of Pathologic Tumor Response and Survival After Preoperative Radiochemotherapy with Bevacizumab in High-Risk Locally Advanced Rectal Cancer. J Nucl Med. 2019;60(11):1560-1568. doi:10.2967/jnumed.118.222604

[55] Wu J, Gensheimer MF, Zhang N, et al. Tumor Subregion Evolution-Based Imaging Features to Assess Early Response and Predict Prognosis in Oropharyngeal Cancer. J Nucl Med. 2020;61(3):327-336. doi:10.2967/jnumed.119.230037

[56] Raica VP, Bratu AM, Zaharia C, Sălcianu IA. CT Evaluation of Squamous Cell Carcinoma of the Nasopharynx. Curr Health Sci J. 2019;45(1):79-86. doi:10.12865/CHSJ.45.01.11

[57] Queiroz MA, Huellner MW. PET/MR in cancers of the head and neck. Semin Nucl Med. 2015;45(3):248-265. doi:10.1053/j.semnuclmed.2014.12.005

[58] Paulus DH, Oehmigen M, Grüneisen J, Umutlu L, Quick HH. Whole-body hybrid imaging concept for the integration of PET/MR into radiation therapy treatment planning. Phys Med Biol. 2016;61(9):3504-3520. doi:10.1088/0031-9155/61/9/3504

[59] Soydal C, Yüksel C, Küçük NÖ, Okten I, Ozkan E, Doğanay Erdoğan B. Prognostic Value of Metabolic Tumor Volume Measured by 18F-FDG PET/CT in Esophageal Cancer Patients. Mol Imaging Radionucl Ther. 2014;23(1):12-15. doi:10.4274/Mirt.07379

[60] Surov A, Stumpp P, Meyer HJ, et al. Simultaneous (18)F-FDG-PET/MRI: Associations between diffusion, glucose metabolism and histopathological parameters in patients with head and neck squamous cell carcinoma. Oral Oncol. 2016;58:14-20. doi:10.1016/j.oraloncology.2016.04.009

[61] Saleh Farghaly HR, Mohamed Sayed MH, Nasr HA, Abdelaziz Maklad AM. Dual time point fluorodeoxyglucose positron emission tomography/computed tomography in differentiation between malignant and benign lesions in cancer patients. Does it always work?. Indian J Nucl Med. 2015;30(4):314-319. doi:10.4103/0972-3919.159693

[62] Helsen N, Van den Wyngaert T, Carp L, Stroobants S. FDG-PET/CT for treatment response assessment in head and neck squamous cell carcinoma: a systematic review and meta-analysis of diagnostic performance. Eur J Nucl Med Mol Imaging. 2018;45(6):1063-1071. doi:10.1007/s00259-018-3978-3

[63] Wong ET, Dmytriw AA, Yu E, et al. 18 F-FDG PET/CT for locoregional surveillance following definitive treatment of head and neck cancer: A meta-analysis of reported studies. Head Neck. 2019;41(2):551-561. doi:10.1002/hed.25513

[64] Qayyum A. Diffusion-weighted imaging in the abdomen and pelvis: concepts and applications. Radiographics. 2009;29(6):1797-1810. doi:10.1148/rg.296095521

[65] Surov A, Meyer HJ, Wienke A. Correlation between apparent diffusion coefficient (ADC) and cellularity is different in several tumors: A meta-analysis. Oncotarget. 2017;8(35):59492-59499.

[66] 1. Hassan O, Taha M shehata, Farag W. Diffusion-weighted MRI versus PET/CT in evaluation of clinically N0 neck in patients with HNSCC. Systematic review and meta-analysis study. Egypt J Ear, Nose, Throat Allied Sci. 2014;15(2):109-116. doi:10.1016/j.ejenta.2014.04.003

[67] Jajodia A, Aggarwal D, Chaturvedi AK, et al. Value of diffusion MR imaging in differentiation of recurrent head and neck malignancies from post treatment changes. Oral Oncol. 2019;96:89-96. doi:10.1016/j.oraloncology.2019.06.037

[68] Martens RM, Noij DP, Koopman T, et al. Predictive value of quantitative diffusion-weighted imaging and 18-F-FDG-PET in head and neck squamous cell carcinoma treated by (chemo)radiotherapy. Eur J Radiol. 2019;113:39-50. doi:10.1016/j.ejrad.2019.01.031

[69] Leifels L, Purz S, Stumpp P, et al. Associations between 18F-FDG-PET, DWI, and DCE Parameters in Patients with Head and Neck Squamous Cell Carcinoma Depend on Tumor Grading. Contrast Media Mol Imaging. 2017;2017:5369625. Published 2017 Oct 19. doi:10.1155/2017/5369625

[70] Castelli J, De Bari B, Depeursinge A, et al. Overview of the predictive value of quantitative 18 FDG PET in head and neck cancer treated with chemoradiotherapy. Crit Rev Oncol Hematol. 2016;108:40-51. doi:10.1016/j.critrevonc.2016.10.009

[71] Deron P, Mertens K, Goethals I, et al. Metabolic tumour volume. Prognostic value in locally advanced squamous cell carcinoma of the head and neck. Nuklearmedizin. 2011;50(4):141-146. doi:10.3413/Nukmed-0367-10-11

[72] Jeong JH, Cho IH, Chun KA, Kong EJ, Kwon SD, Kim JH. Correlation Between Apparent Diffusion Coefficients and Standardized Uptake Values in Hybrid (18)F-FDG PET/MR: Preliminary Results in Rectal Cancer. Nucl Med Mol Imaging. 2016;50(2):150-156. doi:10.1007/s13139-015-0390-9

[73] Sakane M, Tatsumi M, Kim T, et al. Correlation between apparent diffusion coefficients on diffusion-weighted MRI and standardized uptake value on FDG-PET/CT in pancreatic adenocarcinoma. Acta Radiol. 2015;56(9):1034-1041. doi:10.1177/0284185114549825

[74] Yamasaki F, Kurisu K, Satoh K, et al. Apparent diffusion coefficient of human brain tumors at MR imaging. Radiology. 2005;235(3):985-991. doi:10.1148/radiol.2353031338

[75] Young H, Baum R, Cremerius U, et al. Measurement of clinical and subclinical tumour response using [18F]-fluorodeoxyglucose and positron emission tomography: review and 1999 EORTC recommendations. European Organization for Research and Treatment of Cancer (EORTC) PET Study Group. Eur J Cancer. 1999;35(13):1773-1782. doi:10.1016/s0959-8049(99)00229-4

[76] Nishimura G, Komatsu M, Hata M, et al. Predictive markers, including total lesion glycolysis, for the response of lymph node(s) metastasis from head and neck squamous cell carcinoma treated by chemoradiotherapy. Int J Clin Oncol. 2016;21(2):224-230. doi:10.1007/s10147-015-0890-8

[77] Han EJ, O JH, Yoon H, et al. FDG PET/CT response in diffuse large B-cell lymphoma: Reader variability and association with clinical outcome. Medicine (Baltimore). 2016;95(39):e4983. doi:10.1097/MD.0000000000004983

[78] Available at: https://www.r-project.org/.

[79] Available at: https://rpkgs.datanovia.com/ggpubr/.

[80] Available at: https://www.r-bloggers.com/easily-explore-your-data-using-the-summarytools-package/.

[81] Gugić J, Strojan P. Squamous cell carcinoma of the head and neck in the elderly. Rep Pract Oncol Radiother. 2012;18(1):16-25. Published 2012 Aug 10. doi:10.1016/j.rpor.2012.07.014

[82] Chajon E, Lafond C, Louvel G, et al. Salivary gland-sparing other than parotid-sparing in definitive head-and-neck intensity-modulated radiotherapy does not seem to jeopardize local control. Radiat Oncol. 2013;8:132. Published 2013 May 30. doi:10.1186/1748-717X-8-132

[83] Yeh SA. Radiotherapy for head and neck cancer. Semin Plast Surg. 2010;24(2):127-136. doi:10.1055/s-0030-1255330

[84] Hoffmann TK. Systemic therapy strategies for head-neck carcinomas: Current status. GMS Curr Top Otorhinolaryngol Head Neck Surg. 2012;11:Doc03. doi:10.3205/cto000085

[85] Chen YJ, Rath T, Mohan S. PET-Computed Tomography in Head and Neck Cancer: Current Evidence and Future Directions. Magn Reson Imaging Clin N Am. 2018;26(1):37-49. doi:10.1016/j.mric.2017.08.003

[86] Kuwano H, Sumiyoshi K, Sonoda K, et al. Relationship between preoperative assessment of organ function and postoperative morbidity in patients with oesophageal cancer. Eur J Surg. 1998;164(8):581-586. doi:10.1080/110241598750005679

[87] Pak K, Cheon GJ, Nam HY, et al. Prognostic value of metabolic tumor volume and total lesion glycolysis in head and neck cancer: a systematic review and meta-analysis. J Nucl Med. 2014;55(6):884-890. doi:10.2967/jnumed.113.133801

[88] Shen G, Ma H, Liu B, Ren P, Kuang A. Correlation of the apparent diffusion coefficient and the standardized uptake value in neoplastic lesions: a meta-analysis. Nucl Med Commun. 2017;38(12):1076-1084. doi:10.1097/MNM.0000000000000746

[89] Er HÇ, Erden A, Küçük NÖ, Geçim E. Correlation of minimum apparent diffusion coefficient with maximum standardized uptake on fluorodeoxyglucose PET-CT in patients with rectal adenocarcinoma. Diagn Interv Radiol. 2014;20(2):105-109. doi:10.5152/dir.2013.13275

[90] Wong KH, Panek R, Dunlop A, et al. Changes in multimodality functional imaging parameters early during chemoradiation predict treatment response in patients with locally advanced head and neck cancer. Eur J Nucl Med Mol Imaging. 2018;45(5):759-767. doi:10.1007/s00259-017-3890-2.

[91] Surov A, Meyer HJ, Höhn AK, Sabri O, Purz S. Combined Metabolo-Volumetric Parameters of 18F-FDG-PET and MRI Can Predict Tumor Cellularity, Ki67 Level and Expression of HIF 1alpha in Head and Neck Squamous Cell Carcinoma: A Pilot Study. Transl Oncol. 2019;12(1):8-14. doi:10.1016/j.tranon.2018.08.018

7. sz. melléklet

DOKTORI ÉRTEKEZÉS BENYÚJTÁSA ÉS NYILATKOZAT A DOLGOZAT EREDETISÉGÉRŐL

Alulírott

név: Kedves András Gyula

születési név: Kedves András Gyula

anyja neve: Szegedi Emerencia

születési hely, idő: Szekszárd, 1994.12.31.

HIGH-DOSE RADIOTHERAPY PROCEDURES REQUIRING PRECISION, MULTIMODAL IMAGING

című doktori értekezésemet a mai napon benyújtom a(z)

Egészségtudományi Doktori Iskola

ONKOLÓGIA –EGÉSZSÉGTUDOMÁNY, DIAGNOSZTIKAI KÉPALKOTÁS Programjához/témacsoportjához

Témavezető(k) neve: Dr. habil. Kovács Árpád, Dr. habil. Lakosi Ferenc

Egyúttal nyilatkozom, hogy jelen eljárás során benyújtott doktori értekezésemet
- korábban más doktori iskolába (sem hazai, sem külföldi egyetemen) nem nyújtottam be,
- fokozatszerzési eljárásra jelentkezésemet két éven belül nem utasították el,
- az elmúlt két esztendőben nem volt sikertelen doktori eljárásom,
- öt éven belül doktori fokozatom visszavonására nem került sor,
- értekezésem önálló munka, más szellemi alkotását sajátomként nem mutattam be, az irodalmi hivatkozások egyértelműek és teljesek, az értekezés elkészítésénél hamis vagy hamisított adatokat nem használtam.

Dátum: 2022. 12. 12.

.....
doktorjelölt aláírása

.....
témavezető aláírása

.....
társtémavezető aláírása